IDENTIFICATION DES MODÈLES DE RUPTURE DUCTILE TENANT COMPTE DE L'ÉTAT DE CONTRAINTE, DE LA VITESSE DE DÉFORMATION ET DE LA TEMPÉRATURE

Dirk Mohr

Chair of Computational Modeling of Materials in Manufacturing
http://mohr.ethz.ch

ETH Zurich, Switzerland

ETH

Modeling Approaches

Option #3

Non-porous plasticity

+

Damage indicator model

Option #2

Porous plasticity

+

Localization criterion

Option #1

Porous plasticity

+

Coalescence criterion

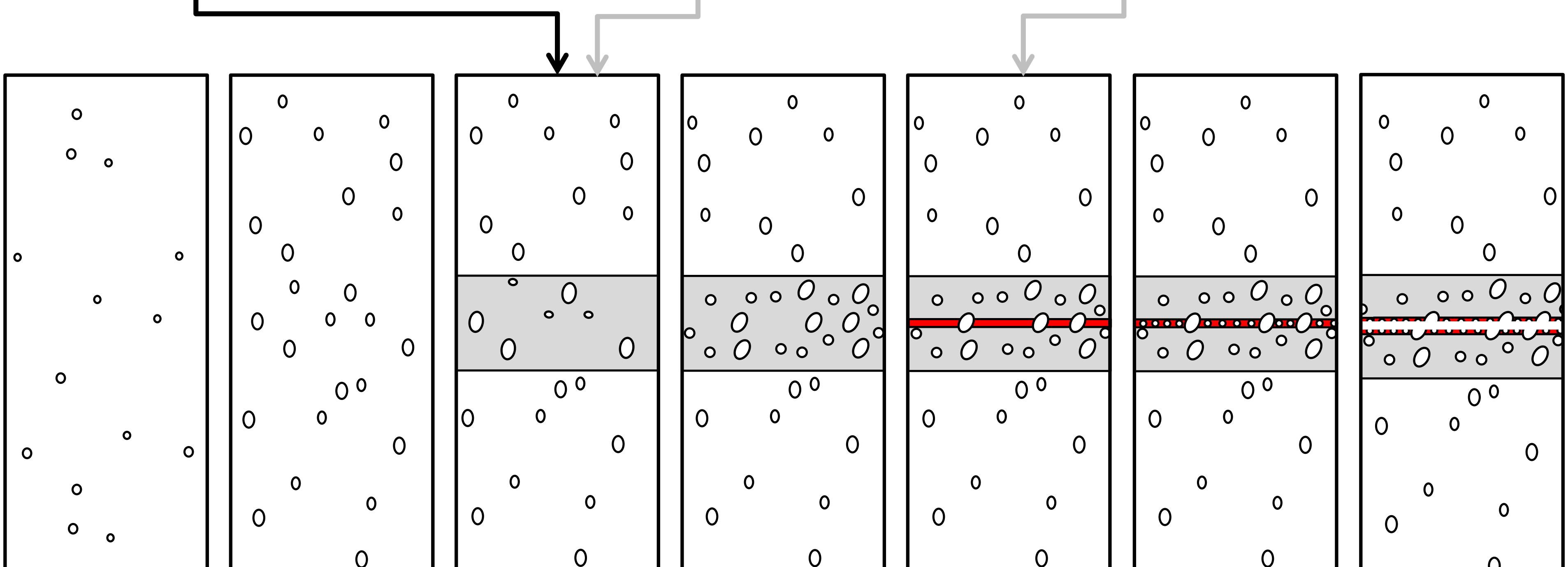

Option #3: Damage Indicator Approach

Chose stress-state dependent fracture criterion such as Cockcroft & Latham (1968), Johnson & Cook (1985), Bai & Wierzbicki (2010), etc

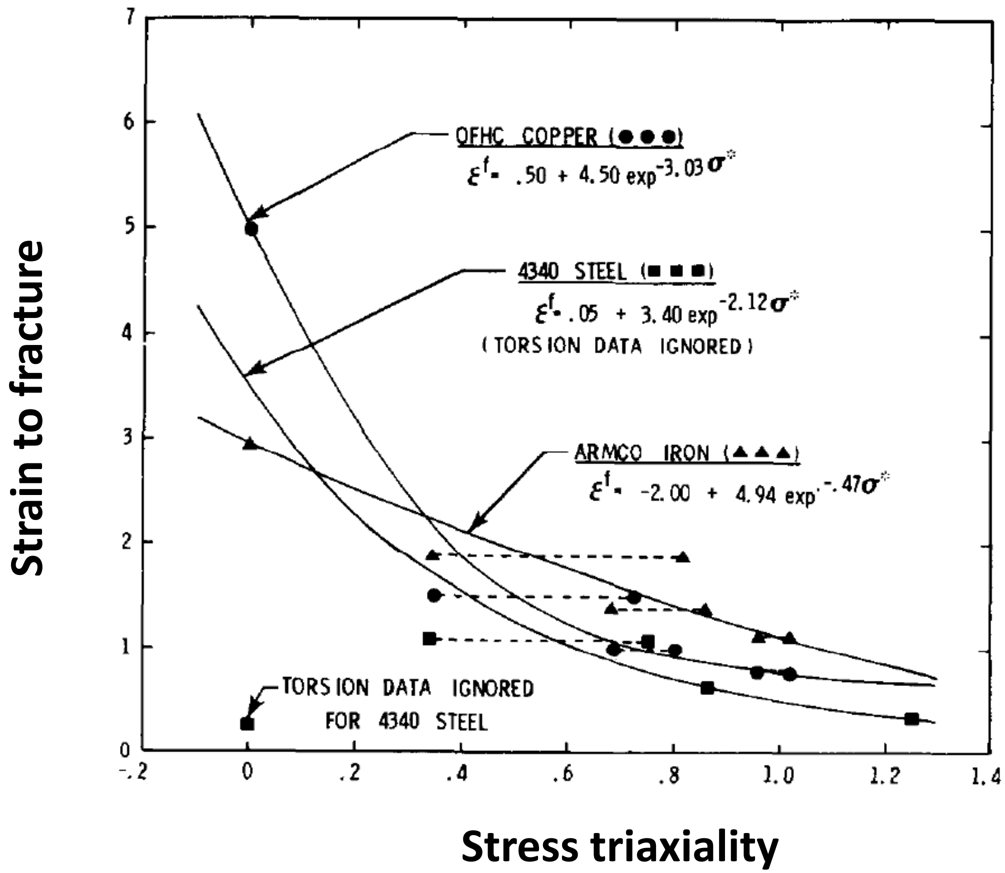

$$\bar{\varepsilon}_f^{pr} = \bar{\varepsilon}_f^{pr}[\eta, \bar{\theta}]$$

$$D = \int \frac{d\bar{\varepsilon}_p}{\bar{\varepsilon}_f^{pr}[\eta, \bar{\theta}]}$$

$D = 0$ (initial)

$D = 1$ (fracture)

Localization Analysis

$$D = \int \frac{d\bar{\varepsilon}_p}{\bar{\varepsilon}_f^{pr}[\eta, \bar{\theta}]}$$

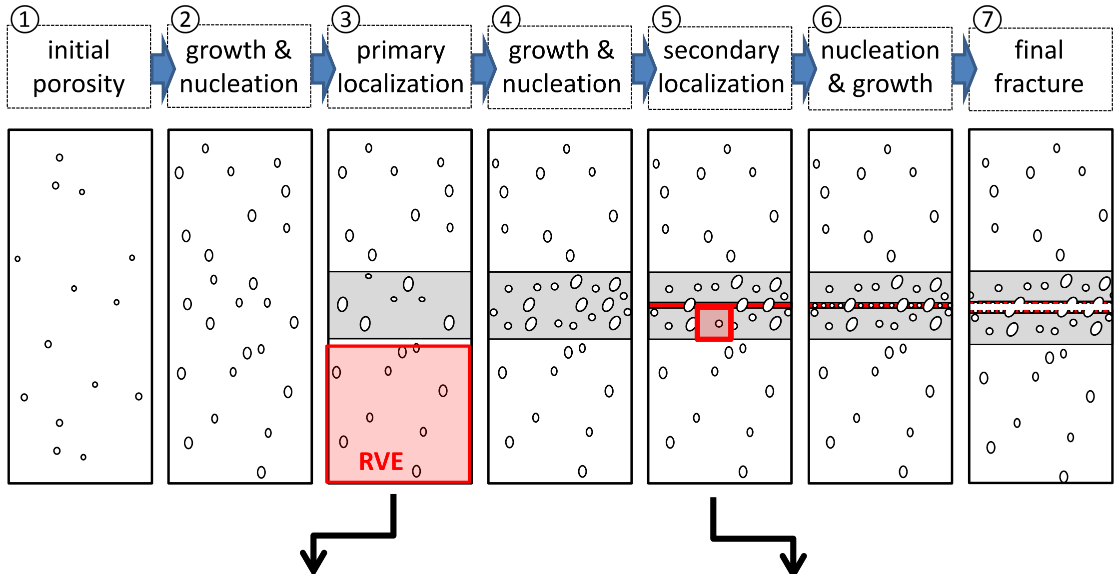

Macroscopic Localization Analysis

- Using Phenomenological porous plasticity
  → Nahshon & Hutchinson (2008)
- Using Homogenization based porous plasticity
  → Danas & Ponte Castaneda (2012)
- Unit cell with random void distribution
  → ongoing

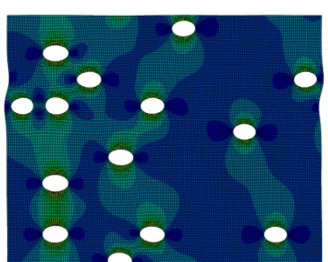

Coalescence Analysis

- Single void unit cell analysis
  → Tvergaard, Pardoen, Needleman, Faleskog, Hopperstad & others
  →
- Analytical criteria
  → e.g. Leblond, Benzerga & others

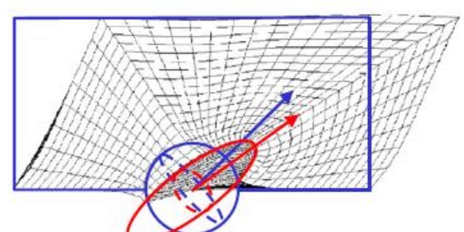

Definition: Lode angle parameter

- Lode number (Lode, 1926)

$$\mu = \frac{2\sigma_{II} - \sigma_I - \sigma_{III}}{\sigma_I - \sigma_{III}}$$

- Lode angle parameter

$$\bar{\theta} = 1 - \frac{2}{\pi}\arccos(\xi) \cong -\mu$$

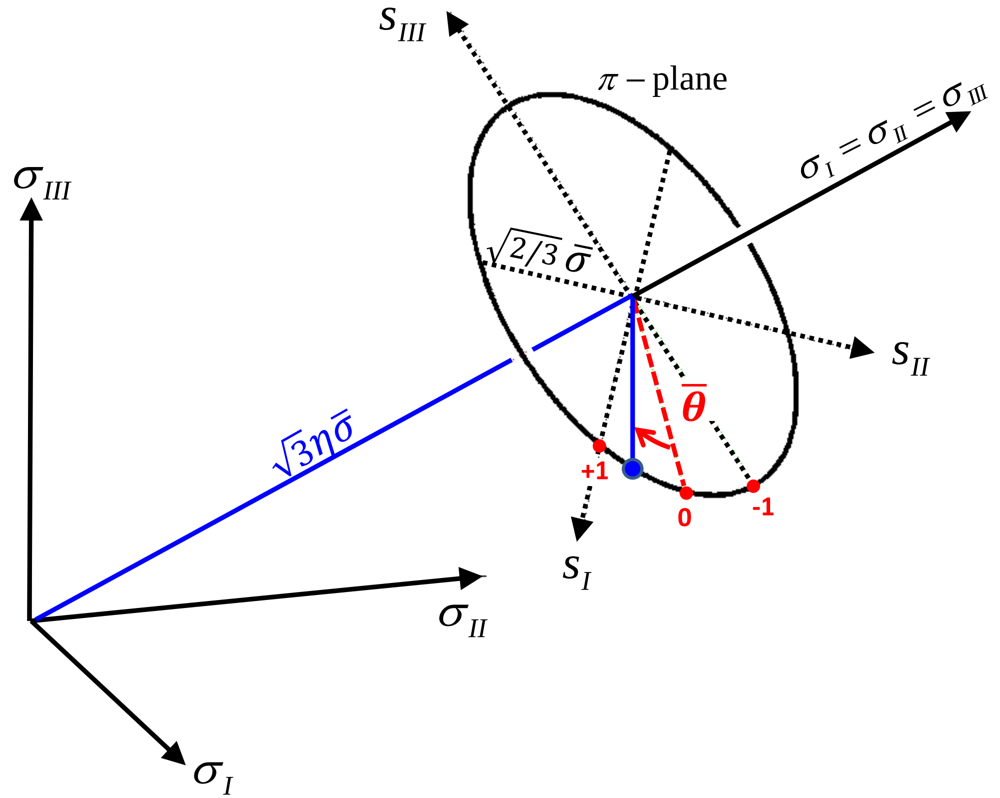

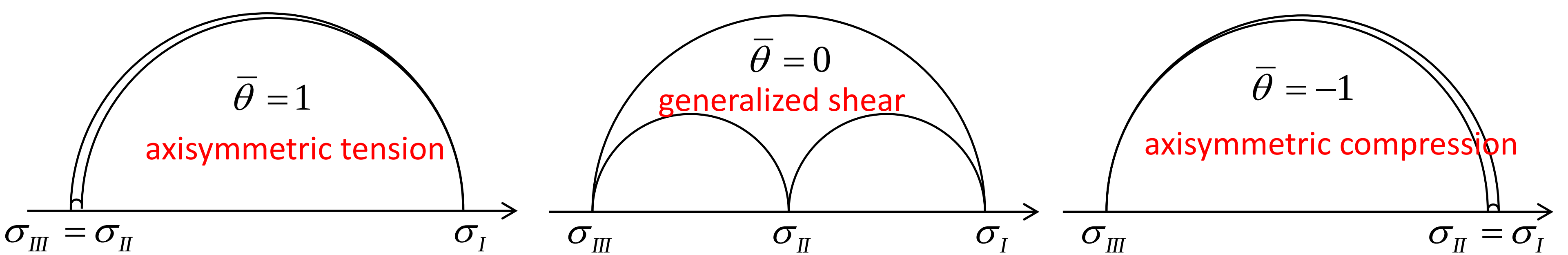

Stress State Map: Unit Cell Analysis

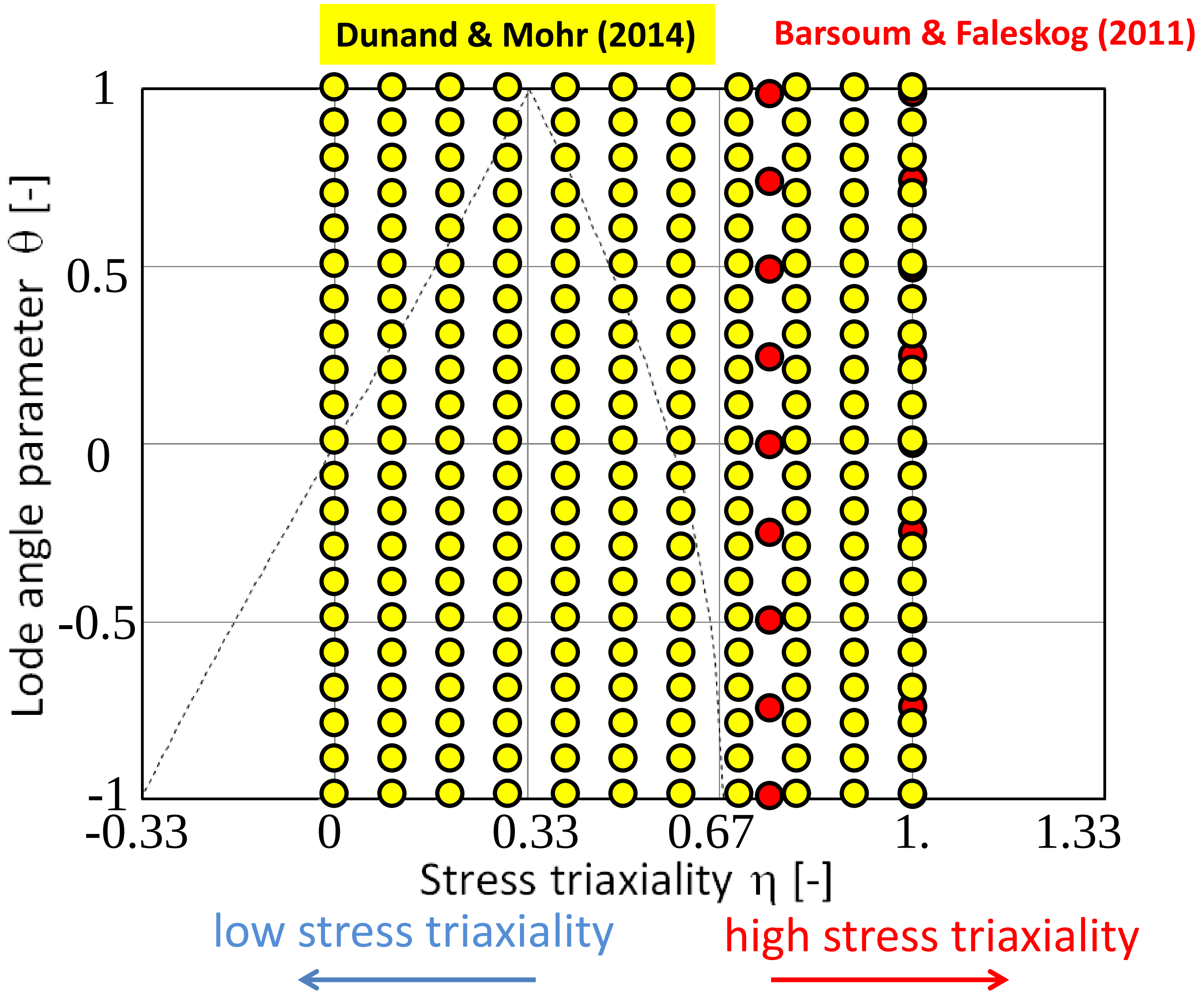

Unit Cell Model

[Dunand and Mohr, JMPS 2014]

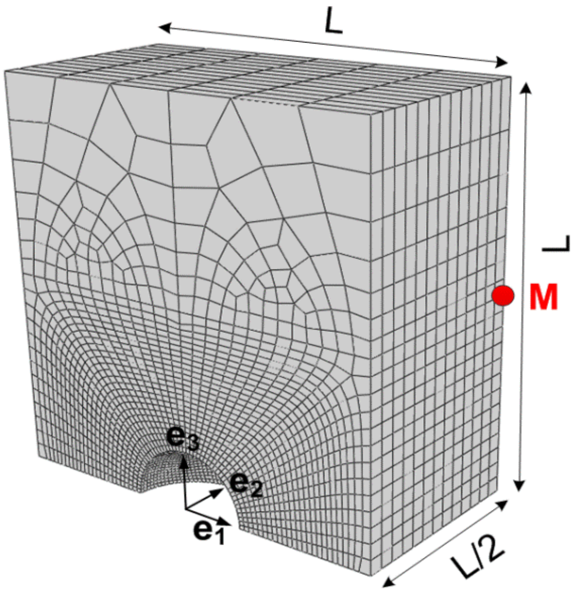

- Matrix material: von Mises with isotropic hardening
- Initial defect volume fraction: 1.2%
- Periodic boundary conditions
- **Macroscopic stress triaxiality and Lode parameter kept constant throughout loading**

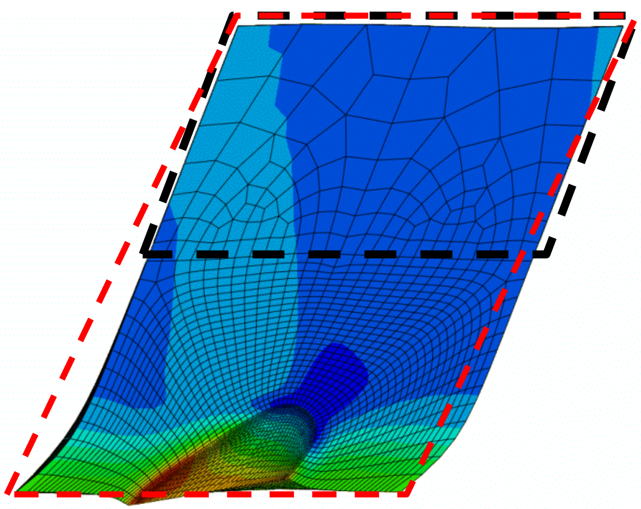

- Kinematic criterion to detect localization

F Deformation gradient of the cell

$\boldsymbol{F^0}$ Deformation gradient outside band of localization

$$\xi = \frac{\|\dot{F}\|}{\|\dot{F}^0\|} \gg 1$$

Needleman & Tvergaard (1992)

Micromechanical Localization Analysis

[Dunand and Mohr, JMPS 2014]

Unit Cell with
Central Void

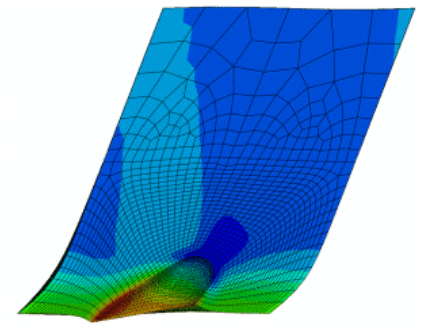

Stresses on
Plane of Localization

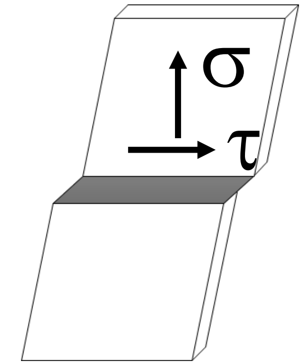

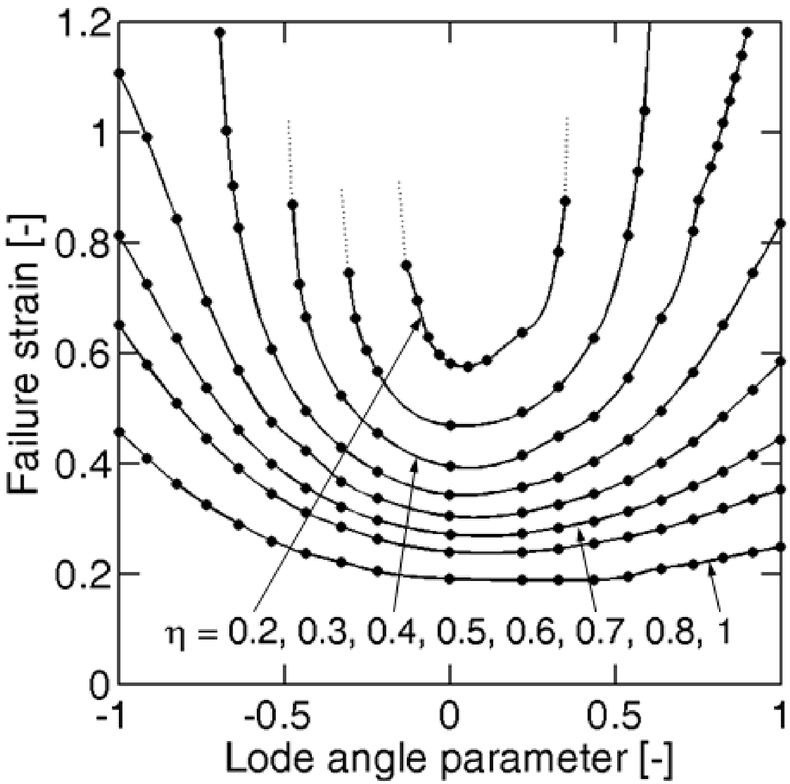

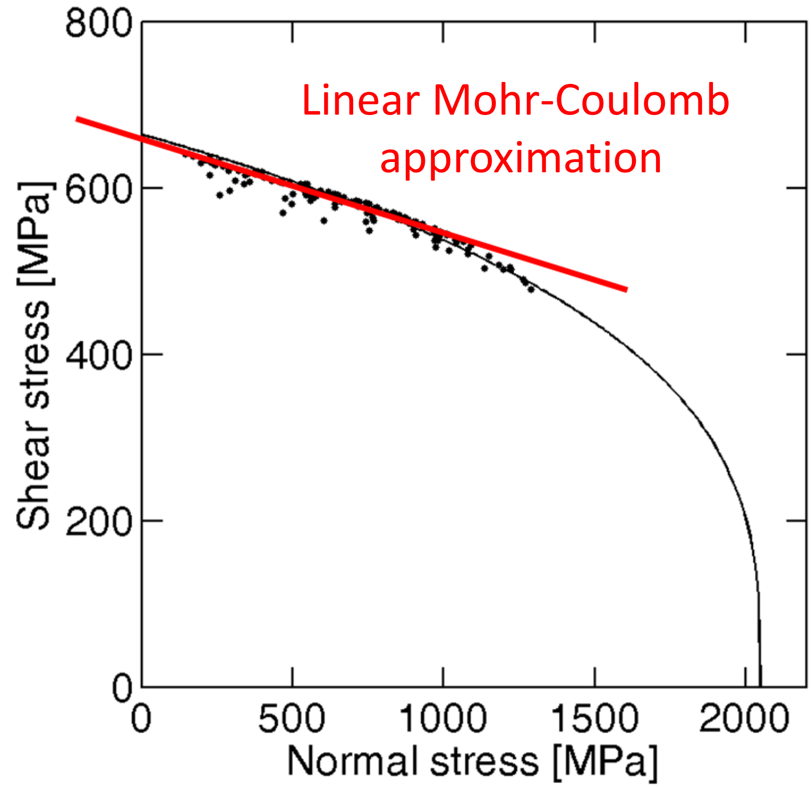

Hosford-Coulomb model

[Mohr and Marcadet, IJSS 2015]

Coordinate transformation

Principal stress space $\{\sigma_I, \sigma_{II}, \sigma_{III}\}$

$$\bar{\sigma} = h(\bar{\theta}, \eta)$$

Haigh-Westergaard space $\{\eta, \bar{\theta}, \bar{\sigma}\}$

Isotropic hardening law

Mixed strain-stress space $\{\eta, \bar{\theta}, \bar{\varepsilon}_p\}$

Hosford-Coulomb

$$\bar{\sigma}_{Hf} + c[\sigma_I + \sigma_{III}] = b$$

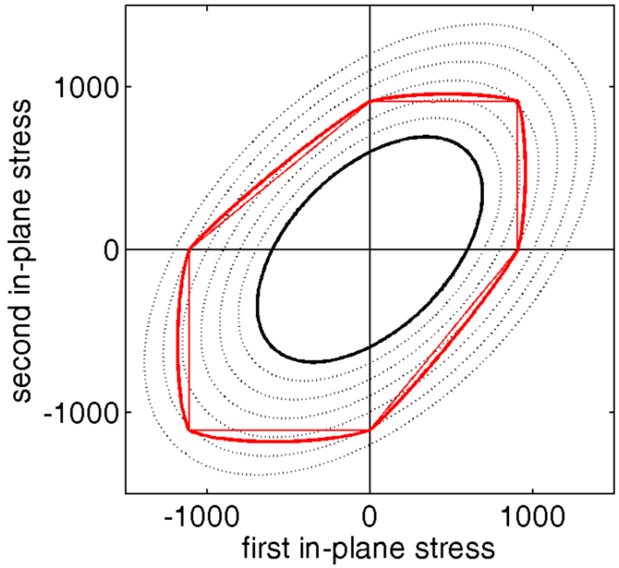

$$\bar{\varepsilon}_p = f(\eta, \bar{\theta})$$

Fracture initiation criterion

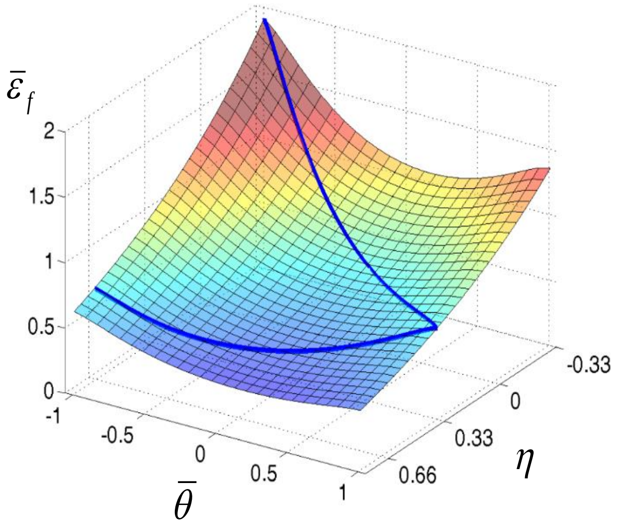

Comparison with Johnson-Cook Failure Model

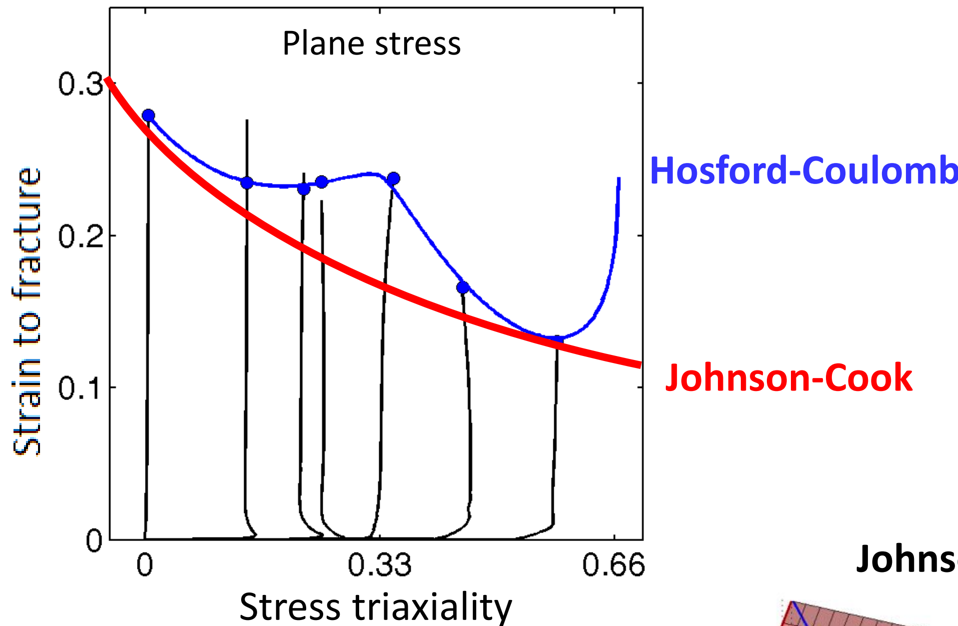

Hosford-Coulomb

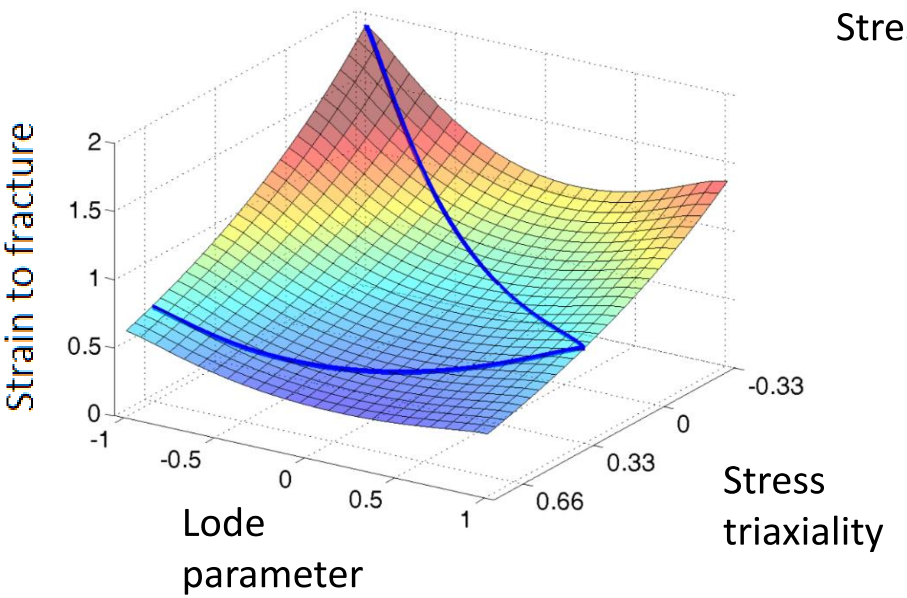

Johnson-Cook

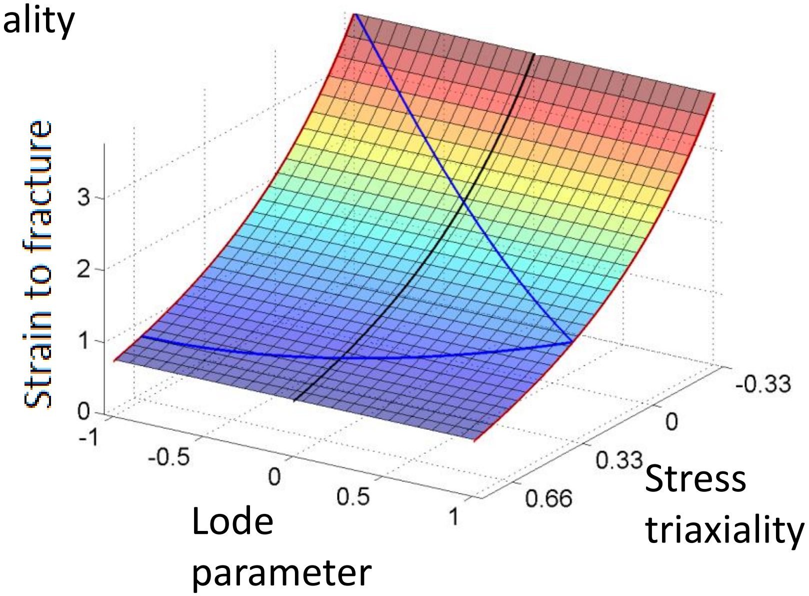

Important Points for Experimental Characterization

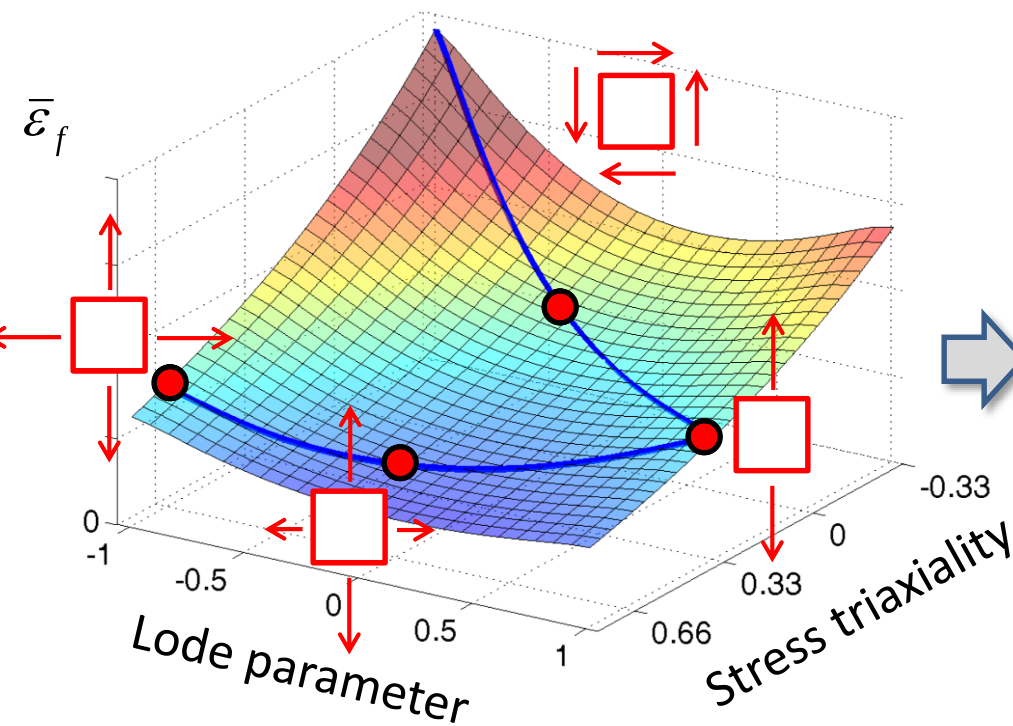

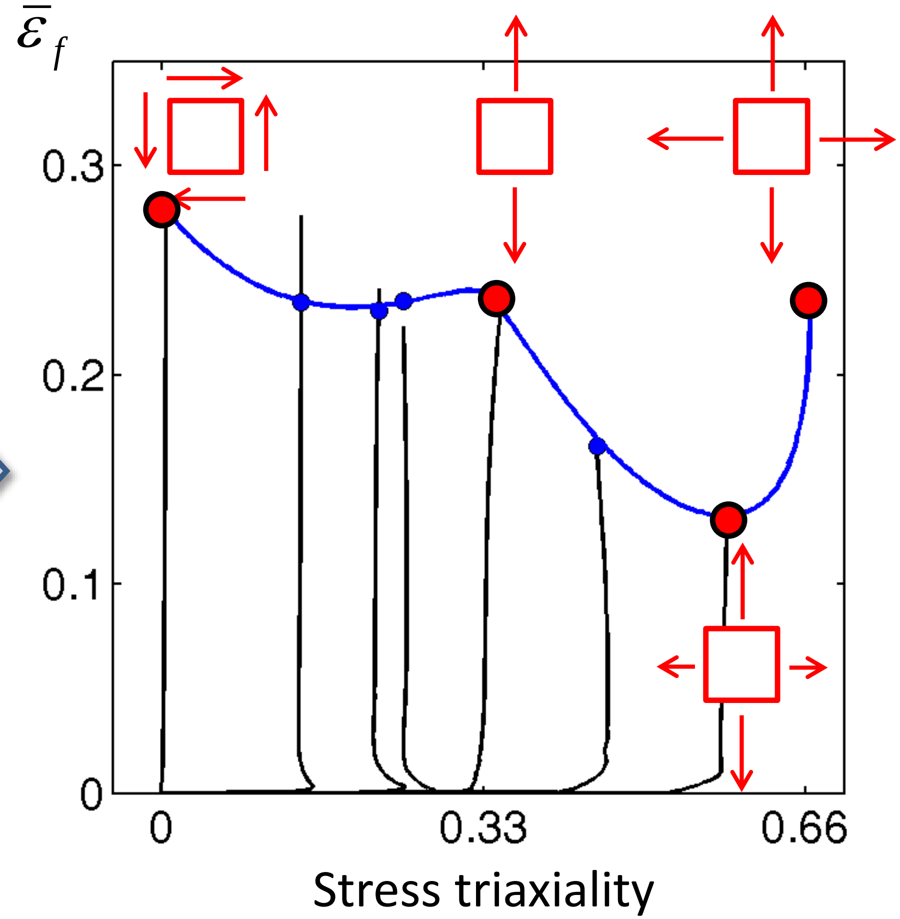

Experiments with Proportional Loading Paths

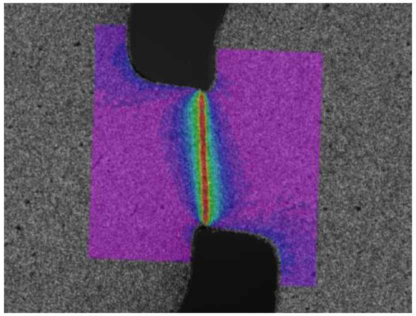

In-plane shear

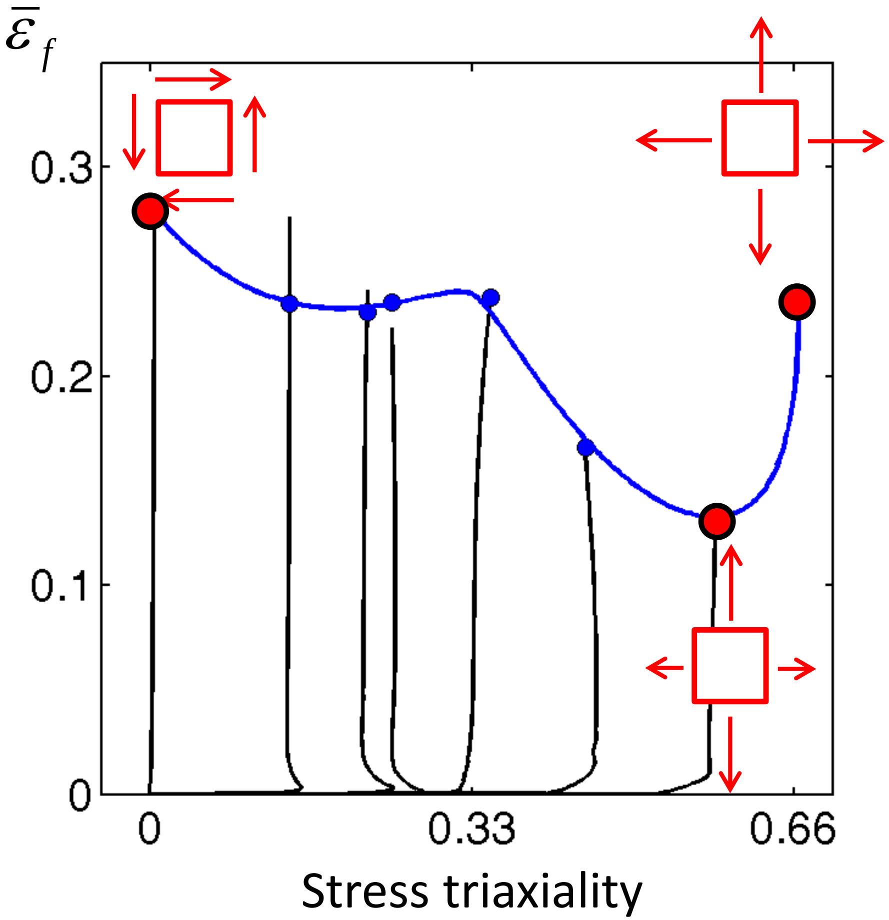

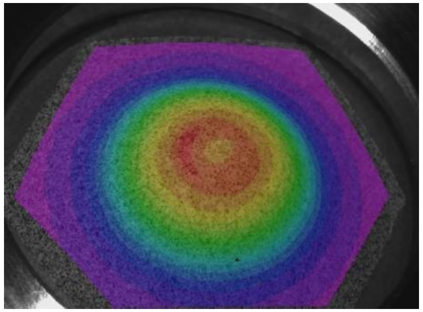

Mini-punch

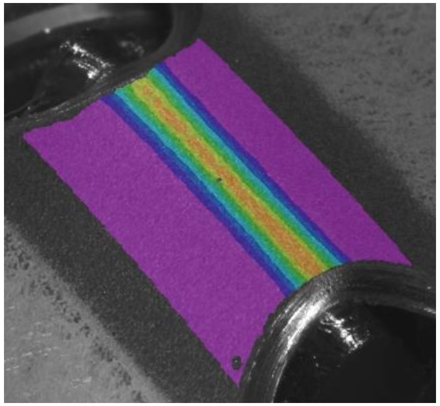

Mini-Nakazima

Plane strain tension: Mini-Nakazima with Dihedral Punch

[Grolleau et al., IJMS 2019]

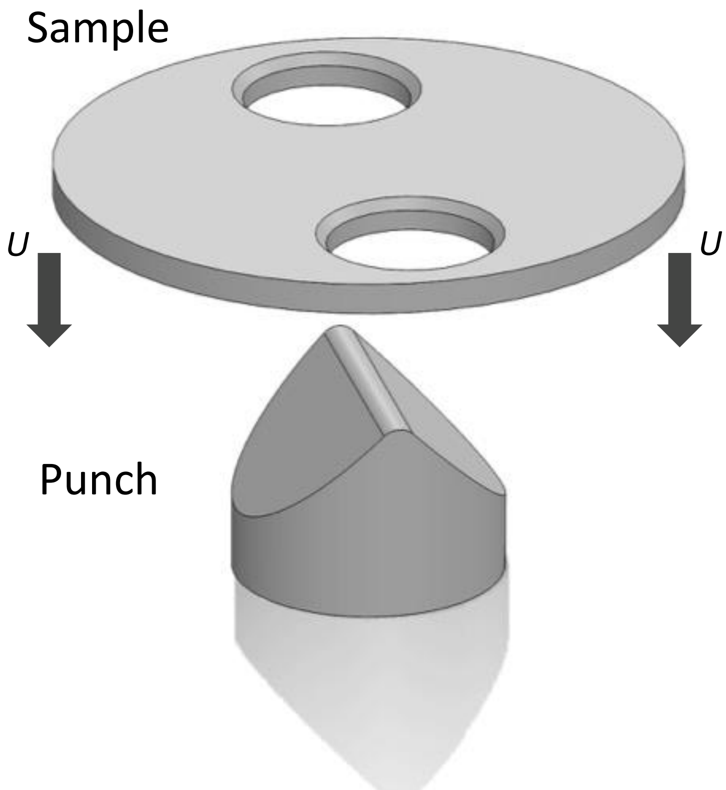

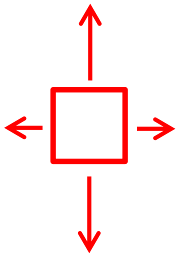

Plane strain tension: Mini-Nakazima with Dihedral Punch

[Grolleau et al., IJMS 2019]

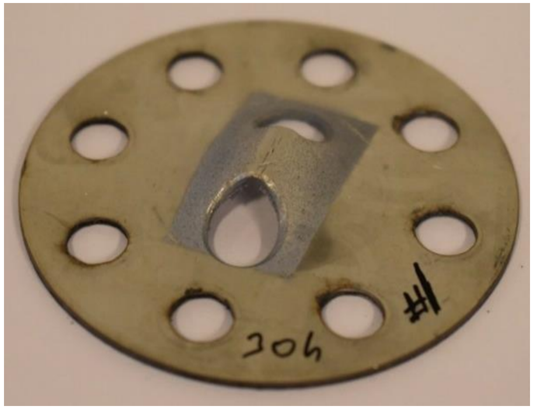

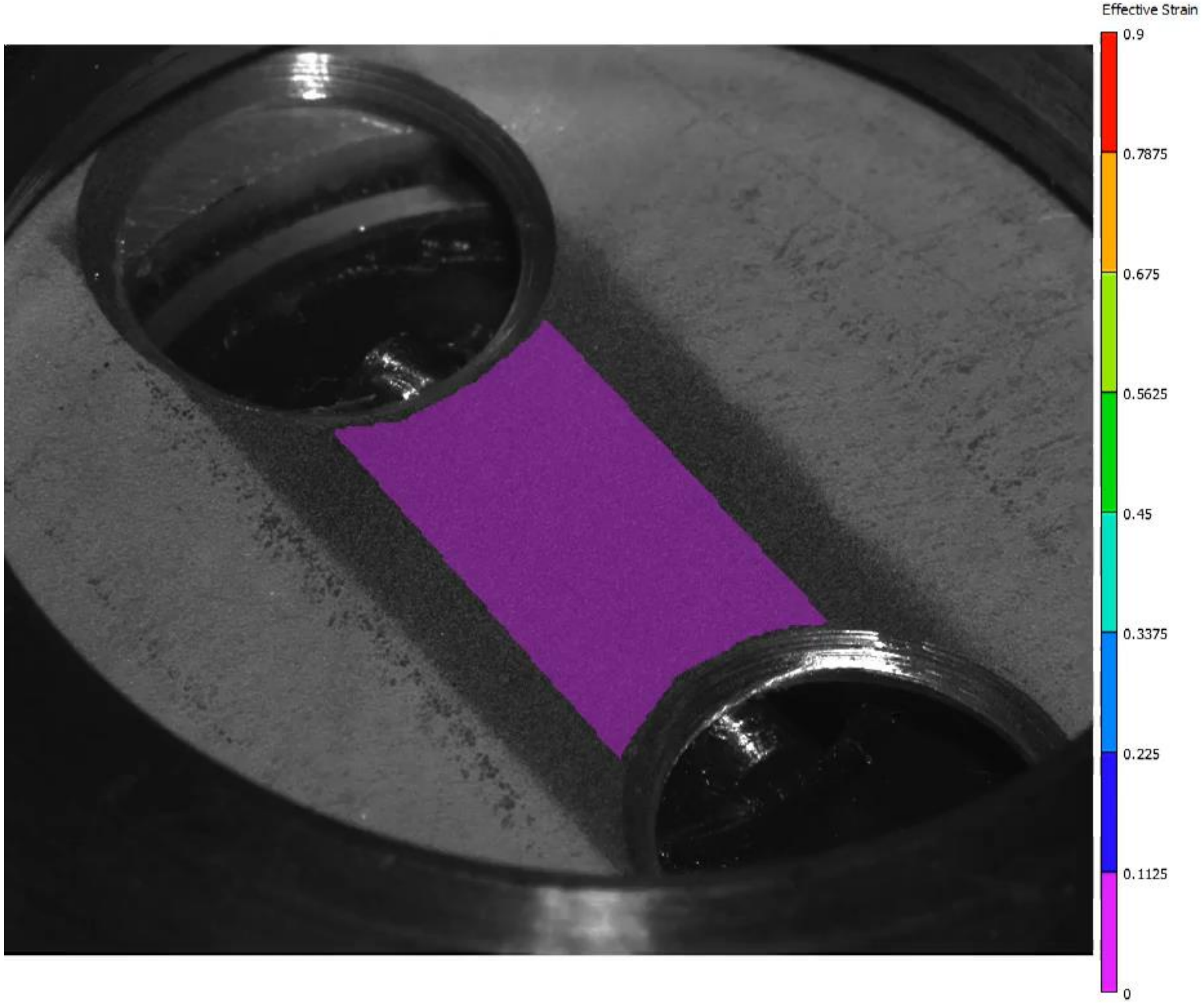

Equi-biaxial tension: mini-punch test

[Roth & Mohr, IJP 2016]

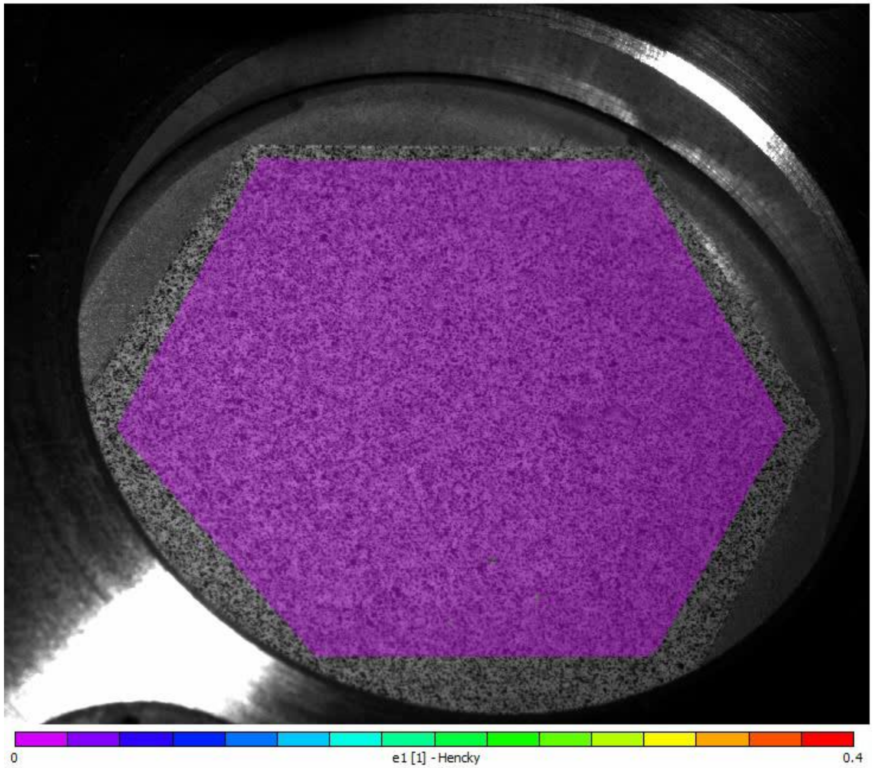

Enhanced Peirs Specimen

[Roth & Mohr, IJMS 2018]

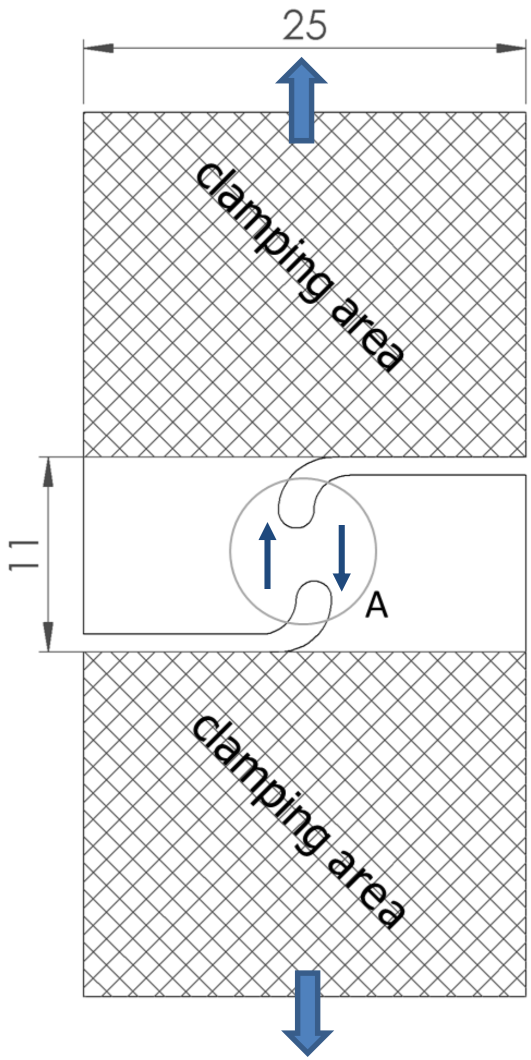

- Optimal geometry depends on material ductility!

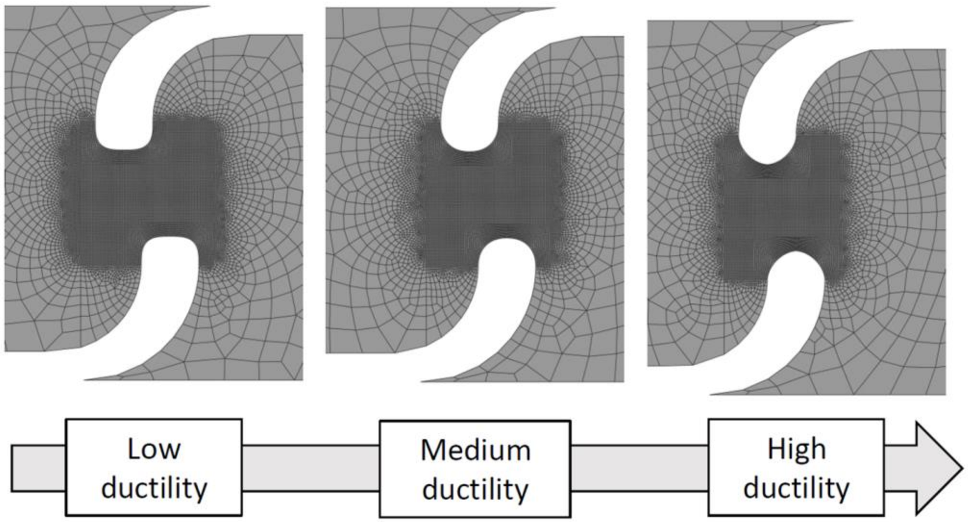

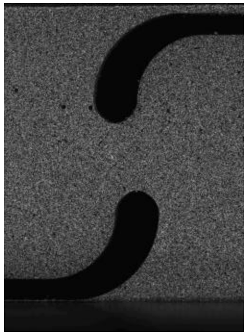

Effects of Strain Rate and Temperature on Ductile Fracture

SHB Tension experiments

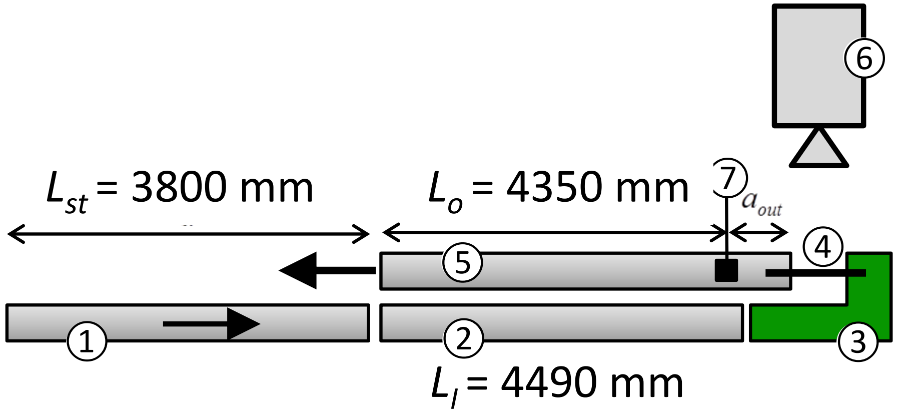

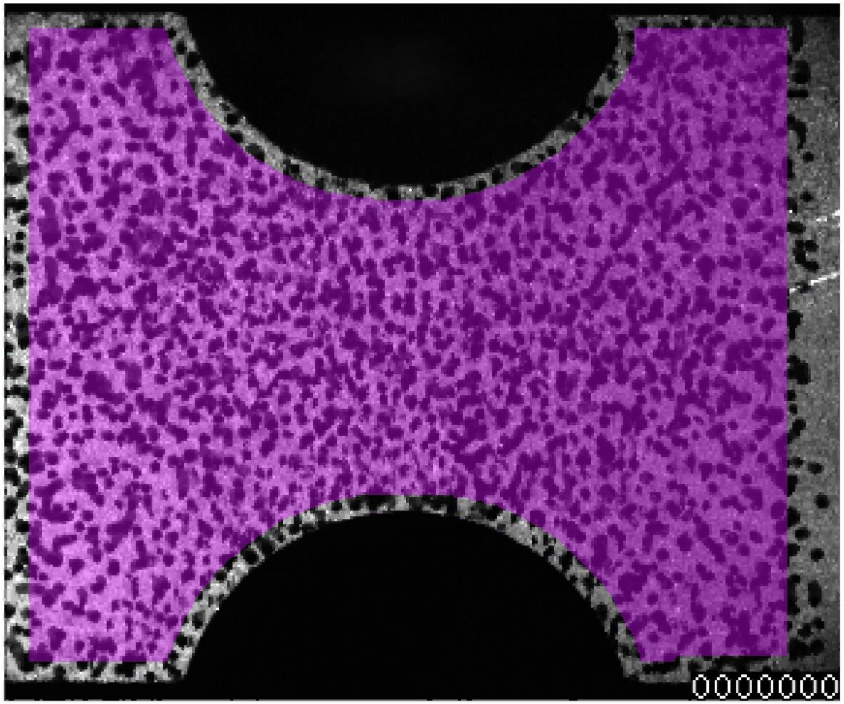

Joint work with Prof. P. Forquin & G. Gary

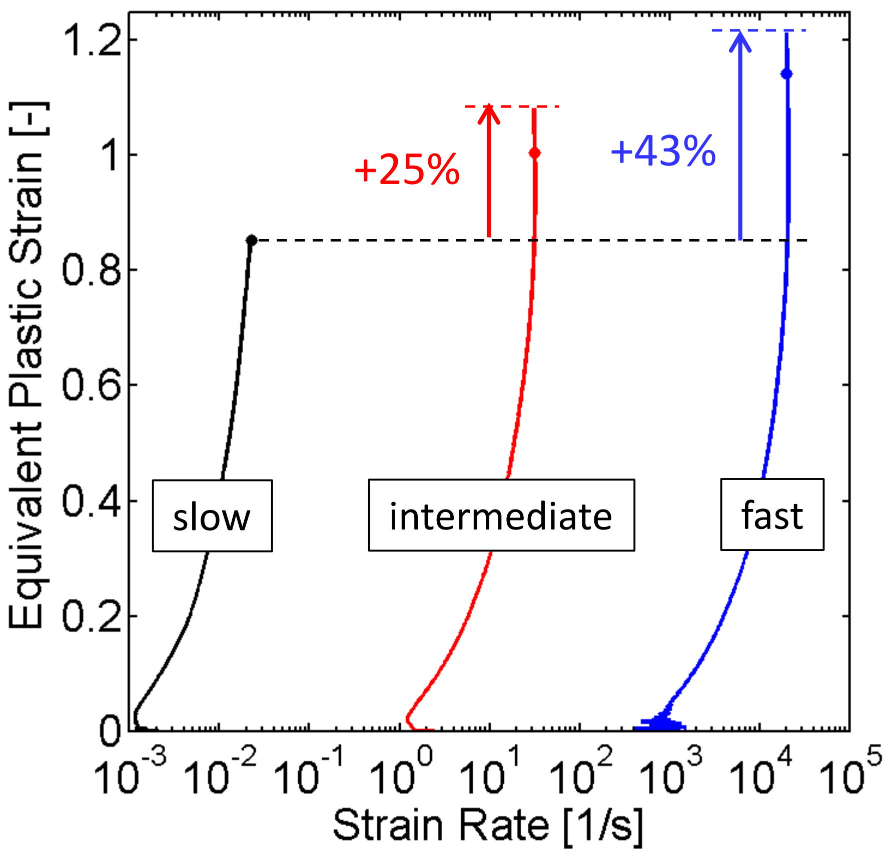

Strain to fracture increases with strain rate!

Rate-dependent Fracture Model

Roth and Mohr (IJP, 2014)

Main assumption: strain to fracture increases with strain rate

- Basis: Hosford-Coulomb Model

$$\bar{\varepsilon}_{f,RD} = \left(1 + \gamma \ln\left[\frac{\dot{\bar{\varepsilon}}_p}{\dot{\varepsilon}_0}\right]\right)\bar{\varepsilon}_{f,RI}$$

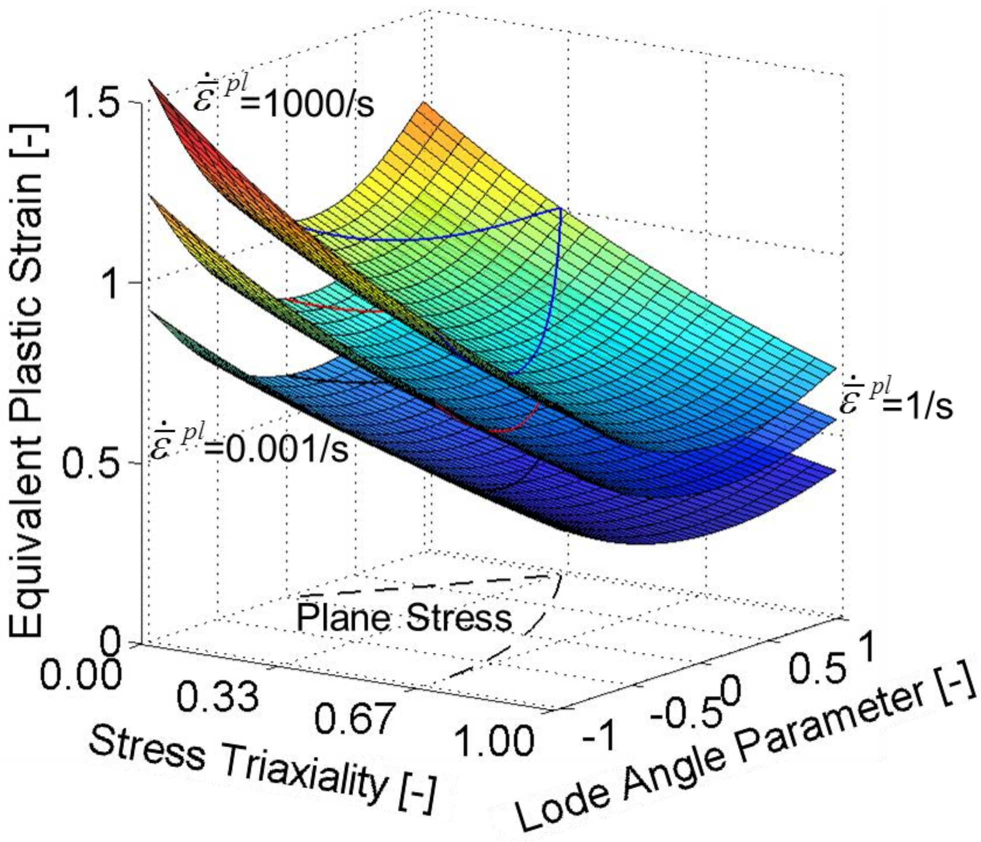

Confirmation for Material #1 (TRIP780)

Roth and Mohr (IJP, 2014)

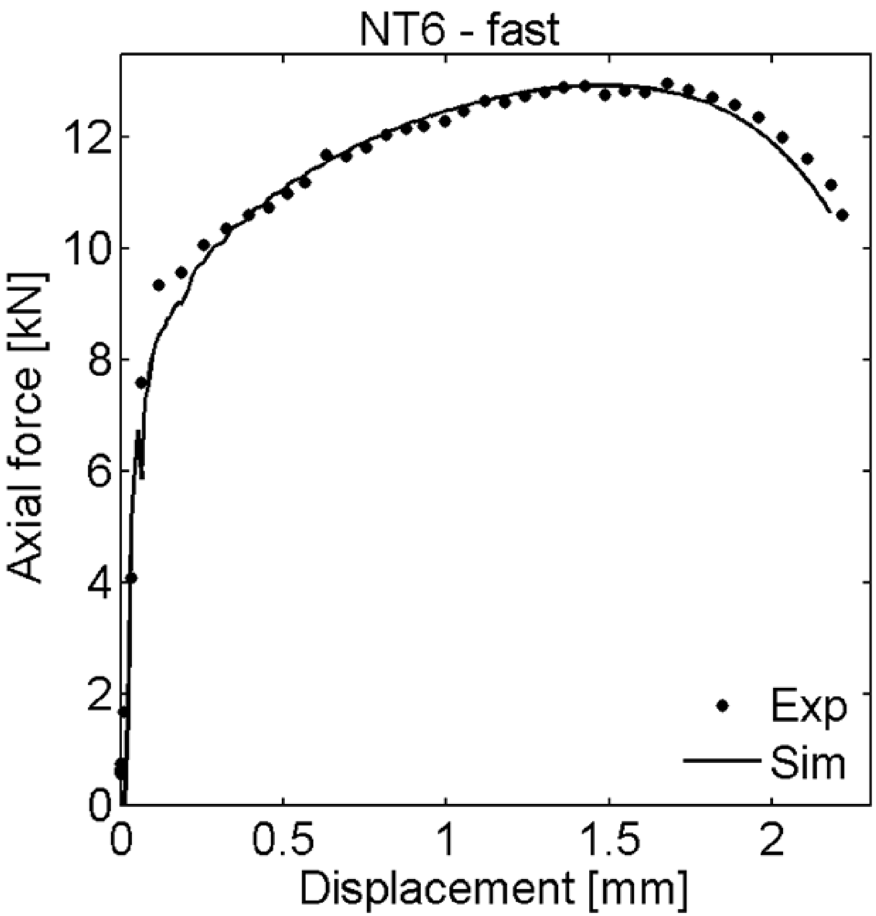

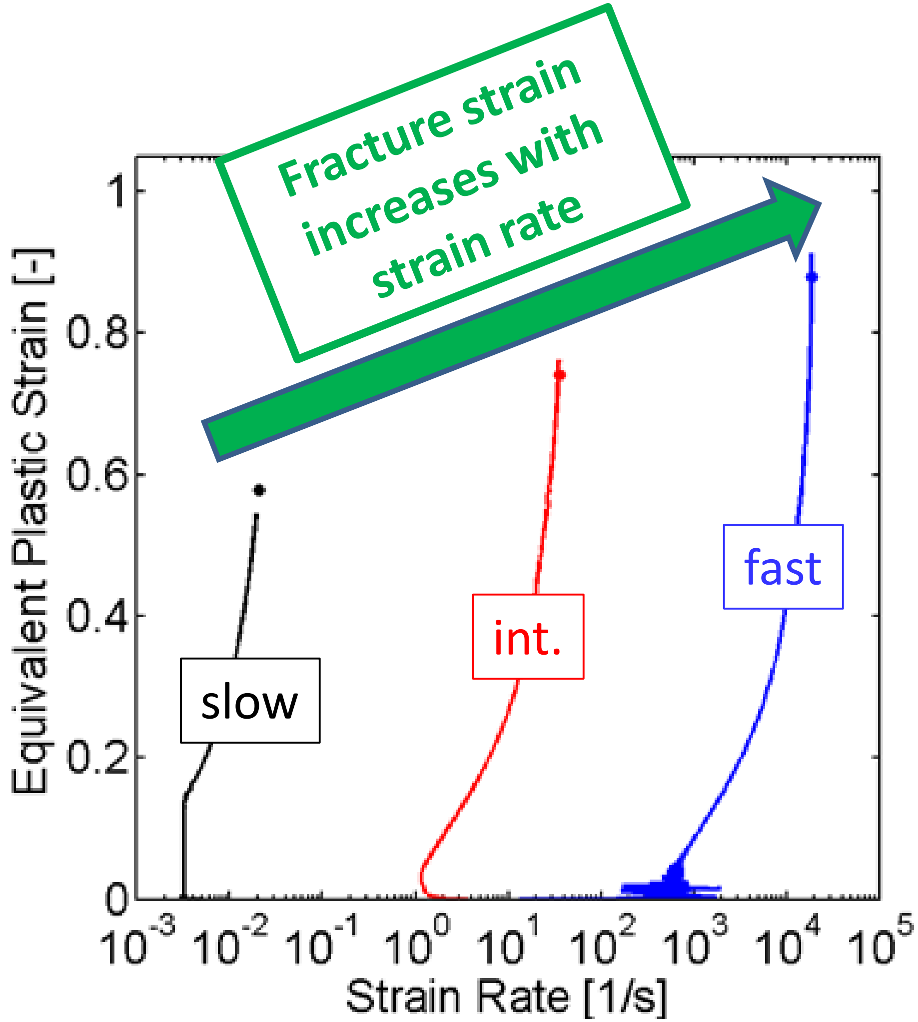

Confirmation for Material #2 (DP980)

Erice, Roth and Mohr (MOM, 2017)

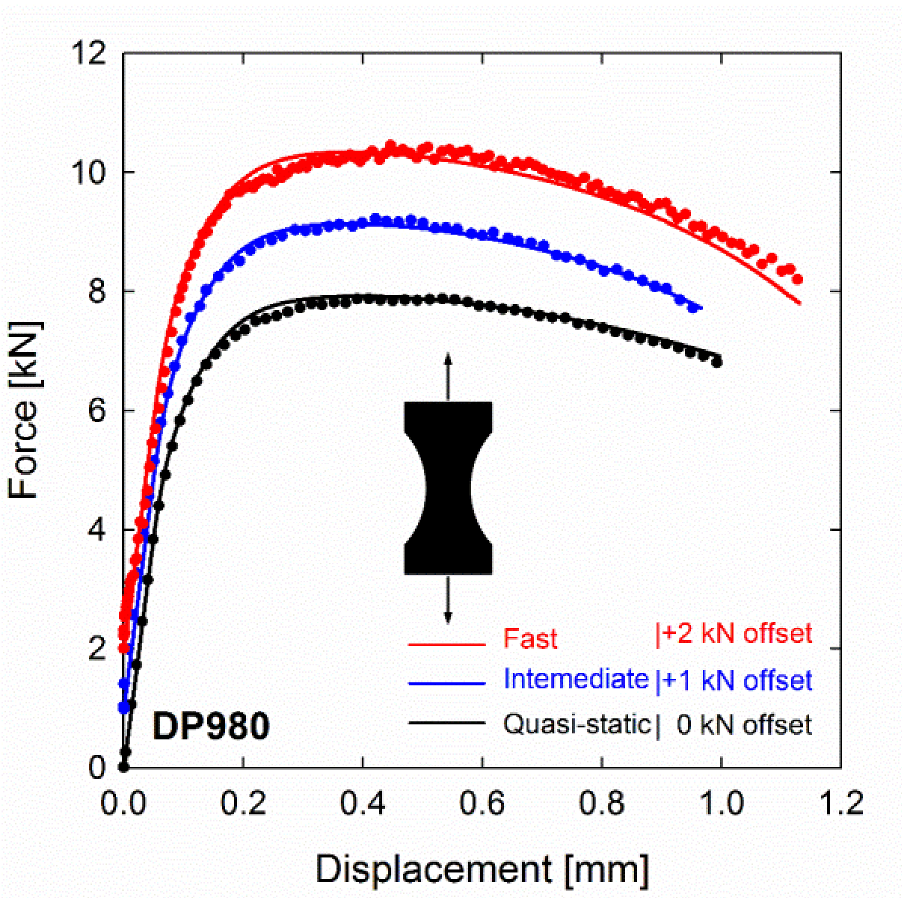

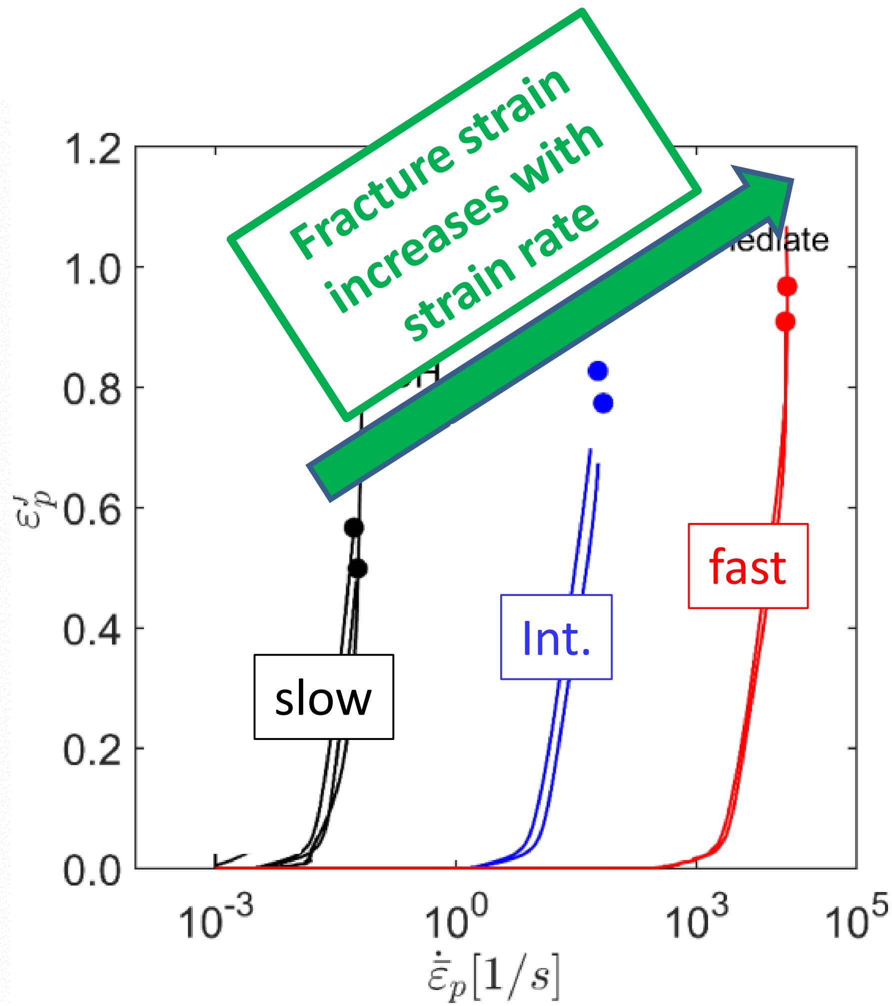

Confirmation for Material #3 (CP1180)

Erice, Roth and Mohr (MOM, 2017)

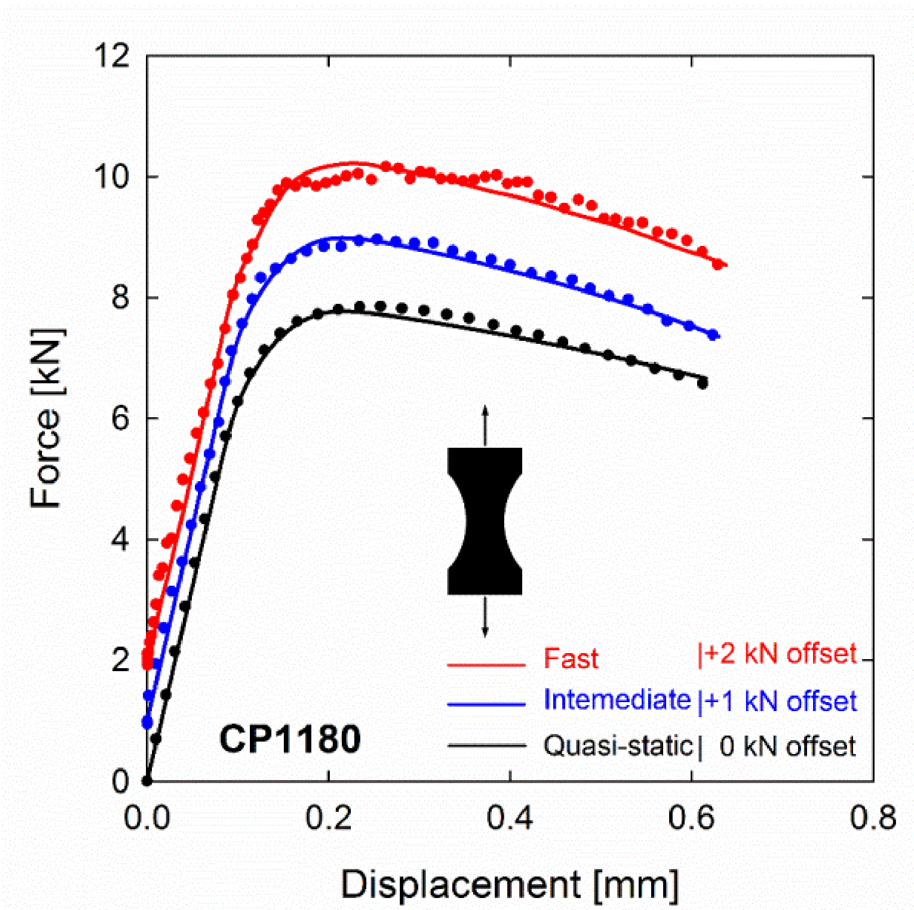

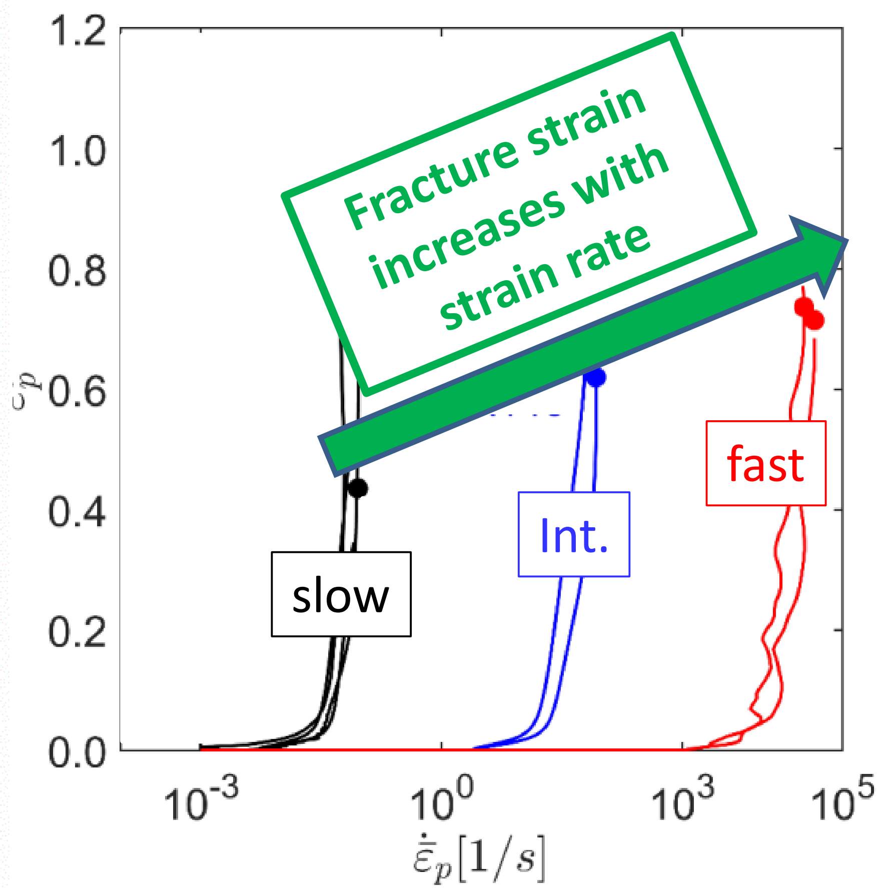

Confirmation for Material #4 (Mars300)

Fras, Roth and Mohr (IJIE, 2018)

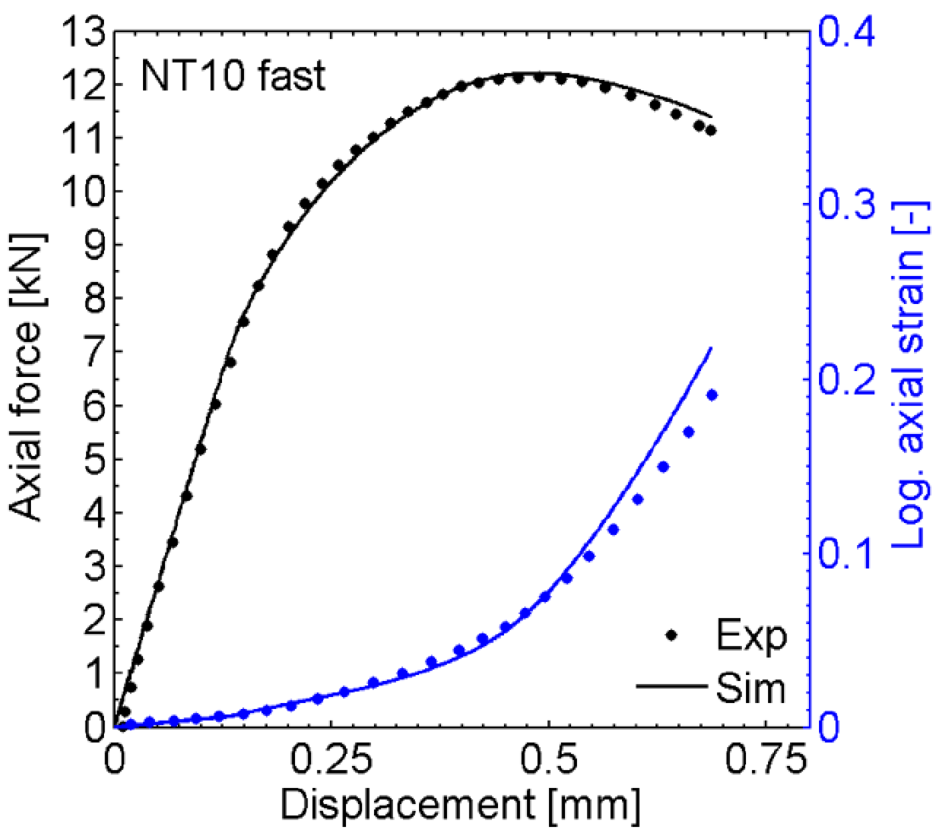

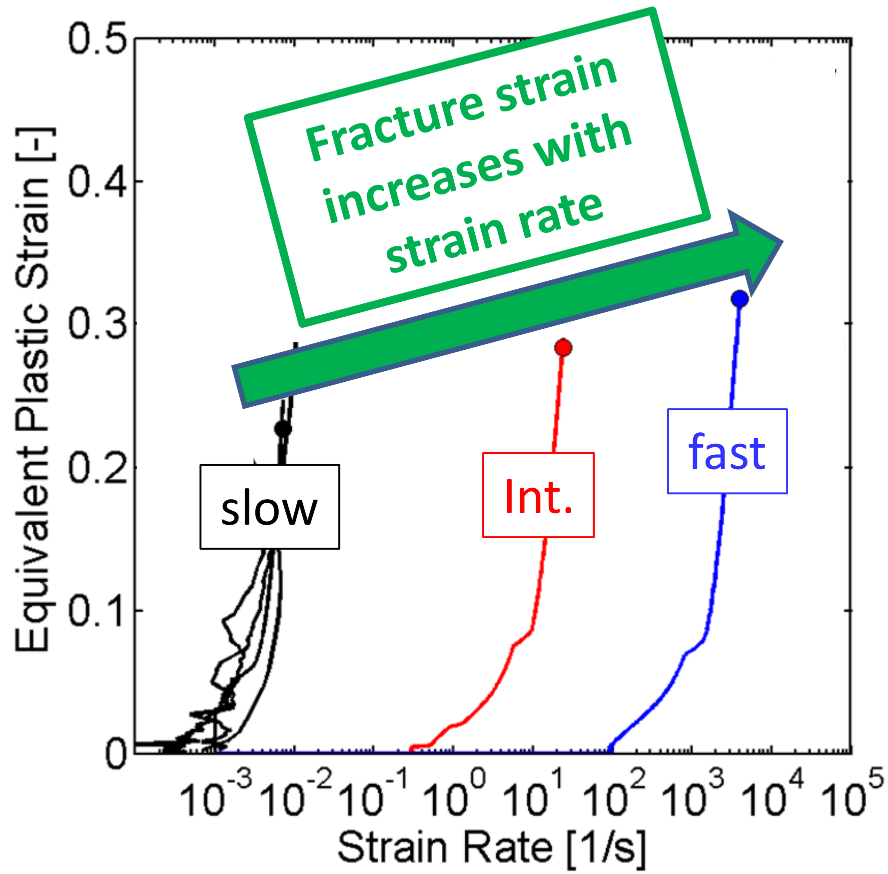

Open Question:

What is the effect of strain rate on fracture strain for pure shear fracture?

3D model

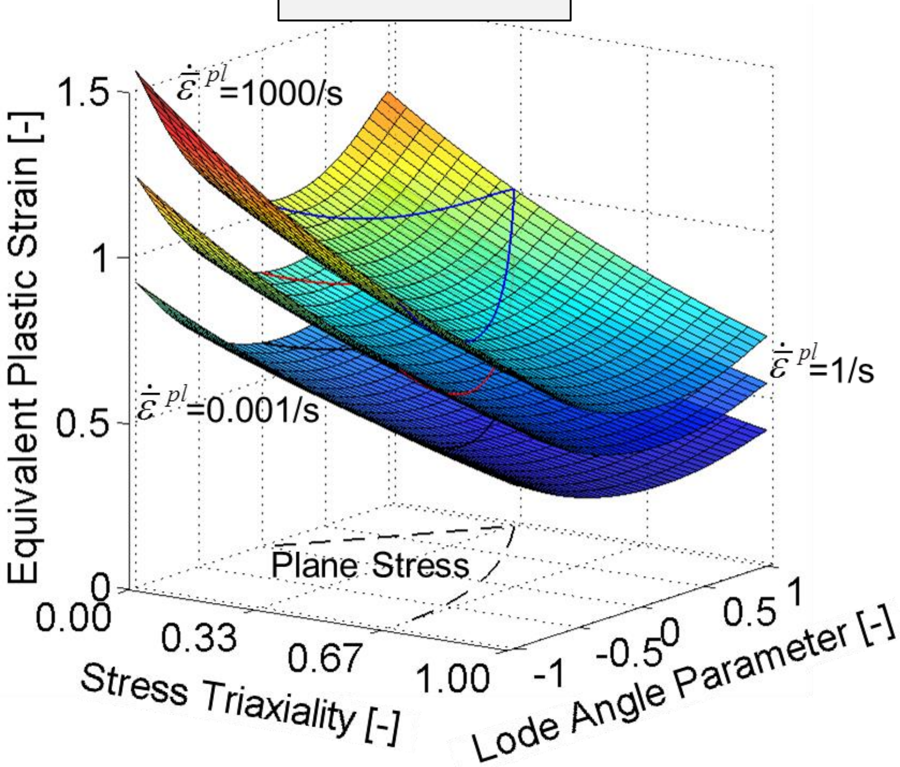

Plane stress model

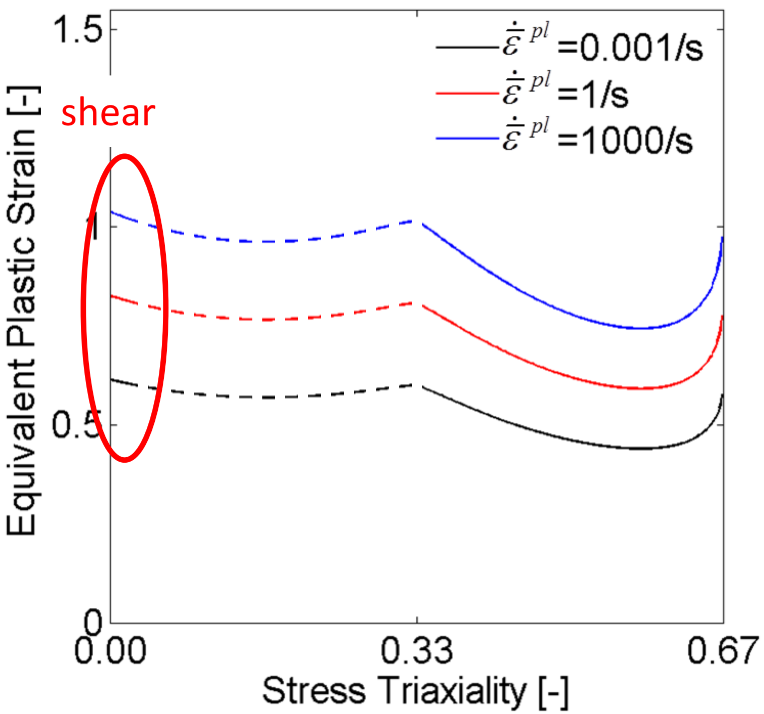

Effect of loading rate on fracture strain

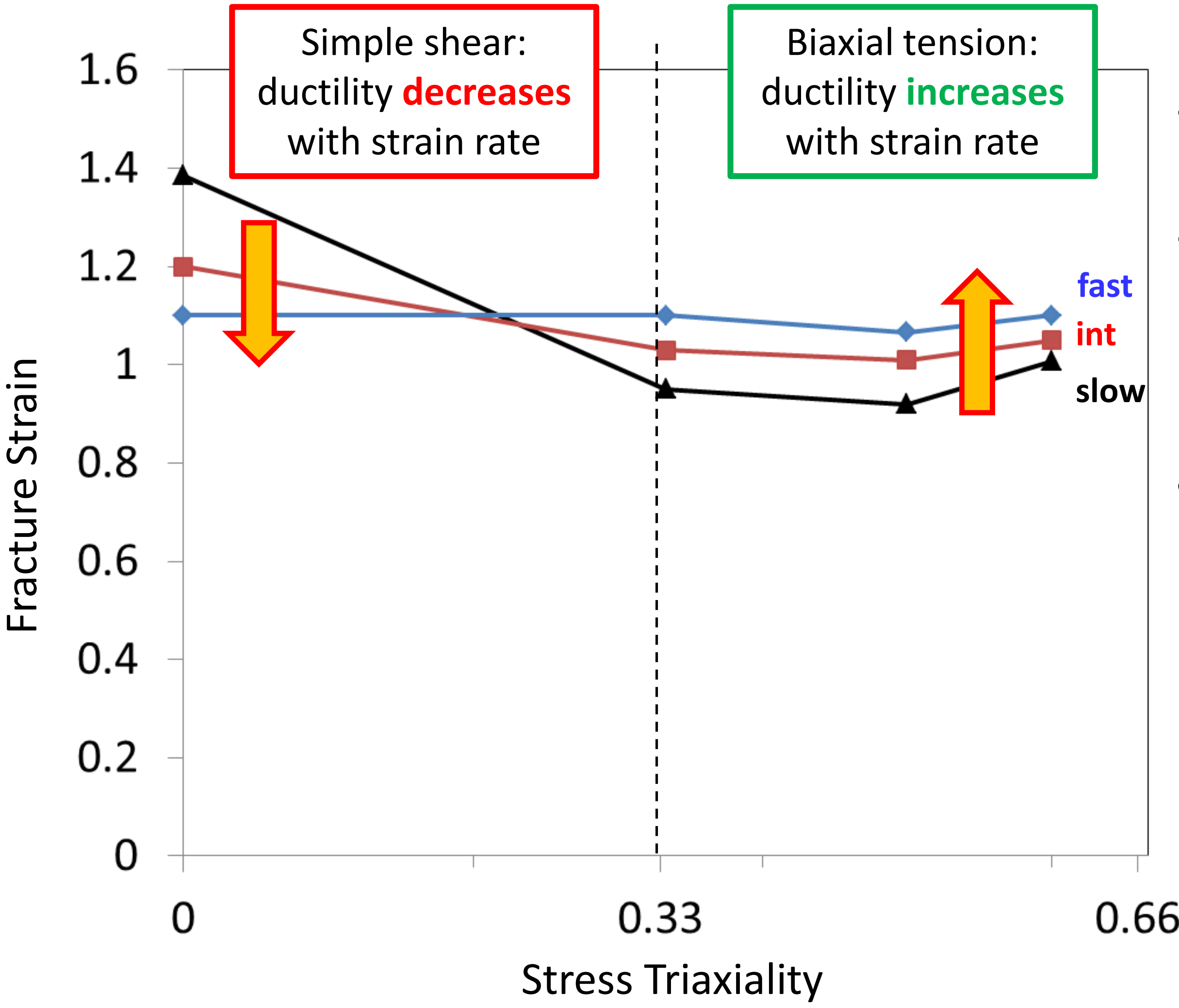

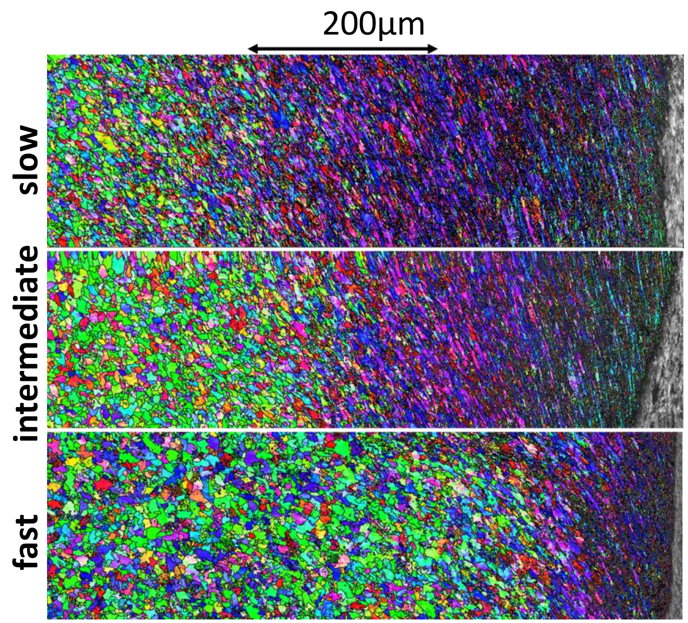

Hypothesis:
Temperature softening effect overwrites increase in ductility due to high strain rate for shear

Experimental setup

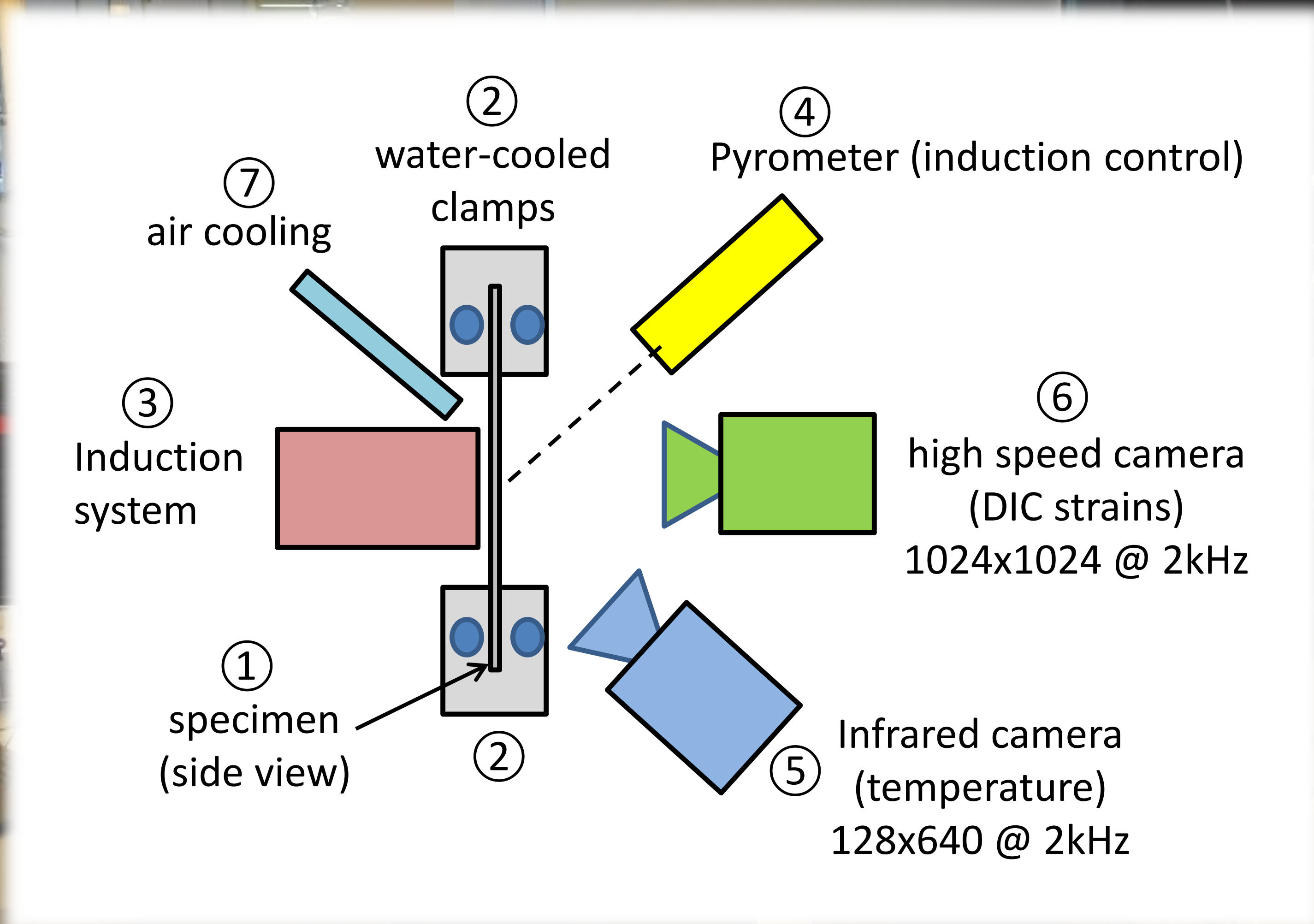

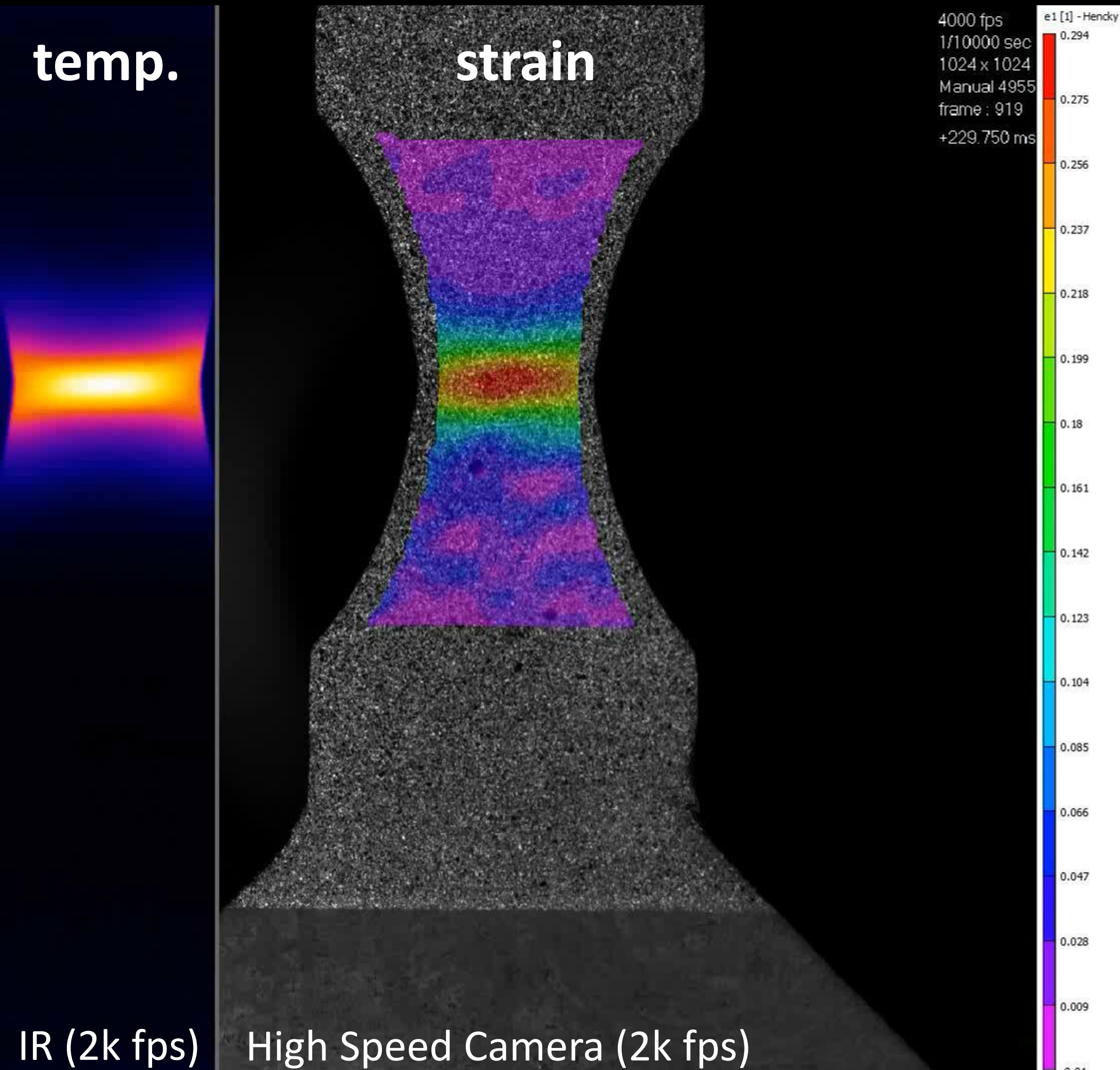
temp.
strain
4000 fps
1/10000 sec
1024 x 1024
Manual 4955
frame : 919
+229.750 ms
e1 [1] - Hencky
0.294
0.275
0.256
0.237
0.218
0.199
0.18
0.161
0.142
0.123
0.104
0.085
0.066
0.047
0.028
0.009
-0.01
IR (2k fps)
High Speed Camera (2k fps)

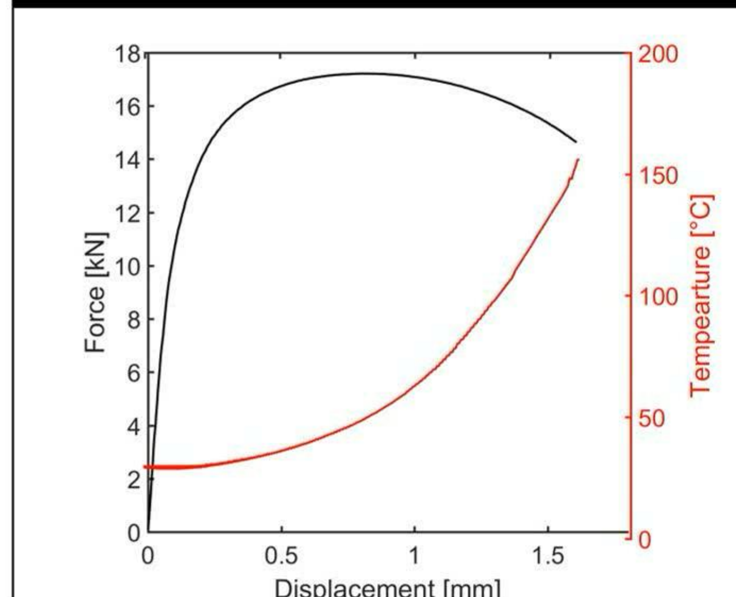
Force [kN]
Tempearture [°C]
Displacement [mm]
0
2
4
6
8
10
12
14
16
18
0
0.5
1
1.5
0
50
100
150
200

Tensile Testing at Elevated Temperatures

Slow @ 6.6 μm/s
(universal testing machine with
induction heating)

Fast @ 3.4m/s
(Hopkinson bar with
induction heating)

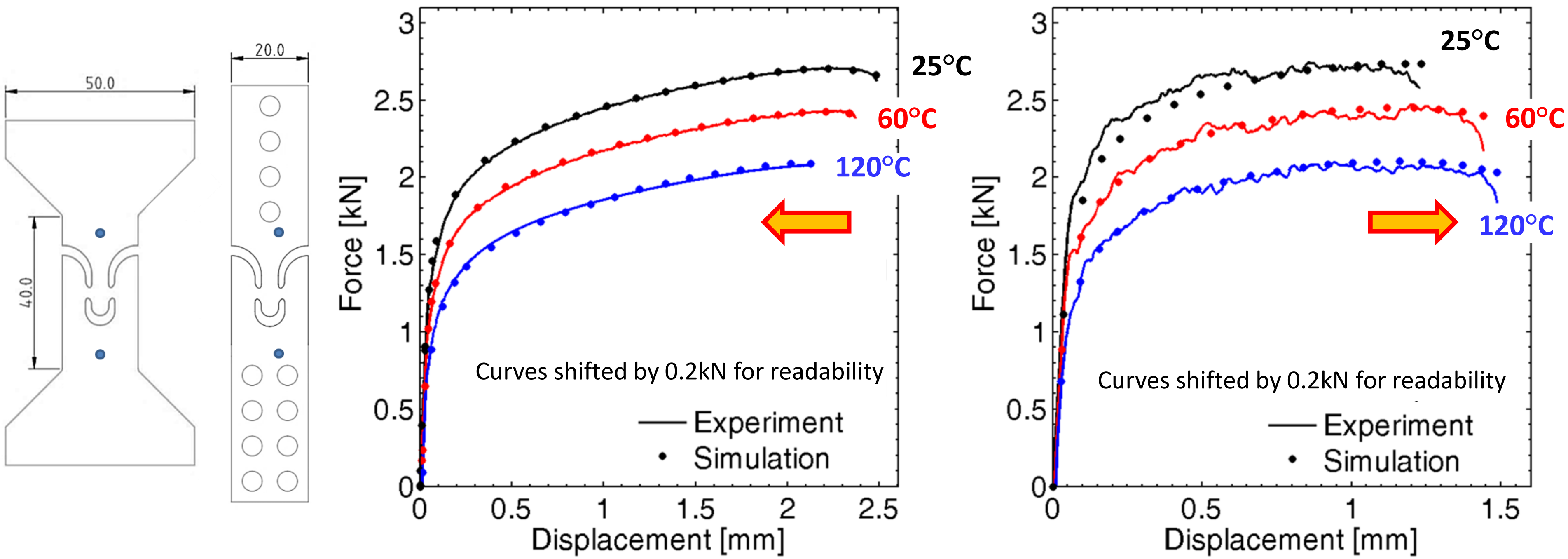

- **Non-monotonic effect of temperature on displacement to fracture**

Quasi-static Experiments from 20 to 300°C

Li, Roth and Mohr (2019)

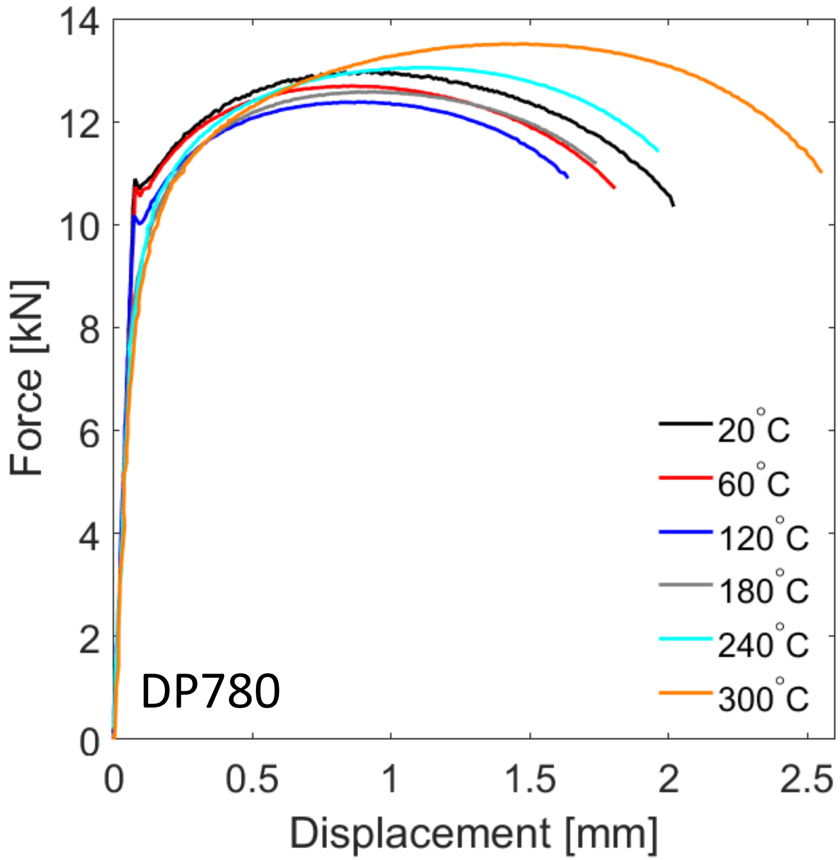

Non-monotonic temperature response on plasticity!

⇨ New plasticity model needed to calculate local fields in fracture specimens!

Machine-Learning Based Johnson-Cook Plasticity Model

Li, Roth and Mohr (2019)

- Johnson-Cook plasticity:

$$\sigma_y = k_1[\overline{\varepsilon_p}] \times k_2[\dot{\overline{\varepsilon_p}}] \times k_3[T]$$

- New approach:

$$\sigma_y = \boxed{k_1[\overline{\varepsilon_p}]} \times \boxed{k_{NN}[\overline{\varepsilon_p}, \dot{\overline{\varepsilon_p}}, T]}$$

Mixed Swift-Voce strain hardening

Scaling factor for temperature and strain rate

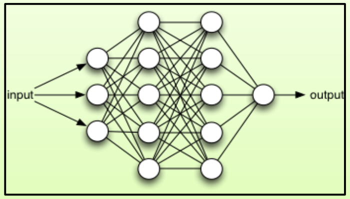

Neural Network

Central Idea:
Introduce a neural network function to describe the effects of strain rate and temperature

Structure of Neural Network

Li, Roth and Mohr (2019)

$$\sigma_y = k_1[\bar{\varepsilon_p}] \times \boxed{k_{NN}[\bar{\varepsilon_p}, \dot{\bar{\varepsilon_p}}, T]}$$

- $k_{NN}[\bar{\varepsilon_p}, \dot{\bar{\varepsilon_p}}, T]$ feedforward network with 10:10:10 structure

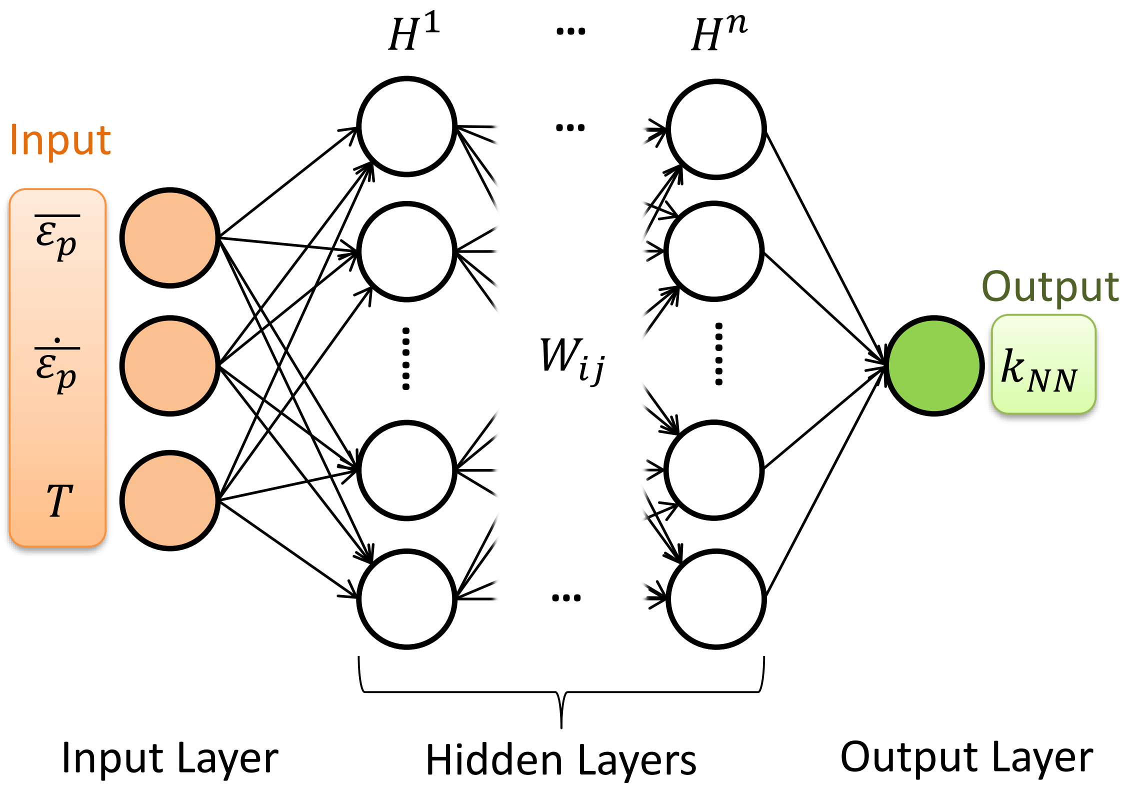

Implemented into user subroutine for Abaqus/Explicit

Performance of Trained Model

Li, Roth and Mohr (2019)

- Training data for loading @ room temperature (three experiments)

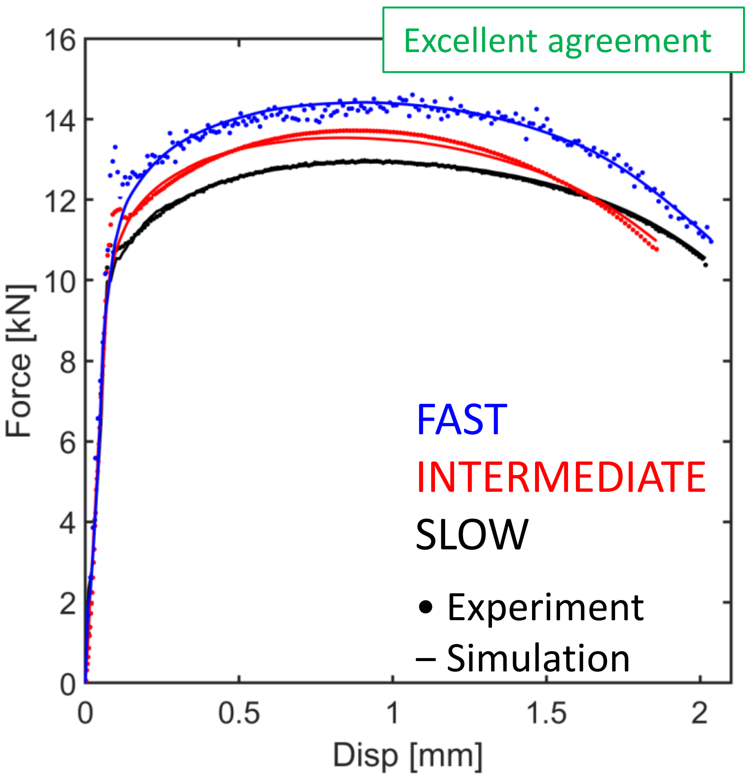

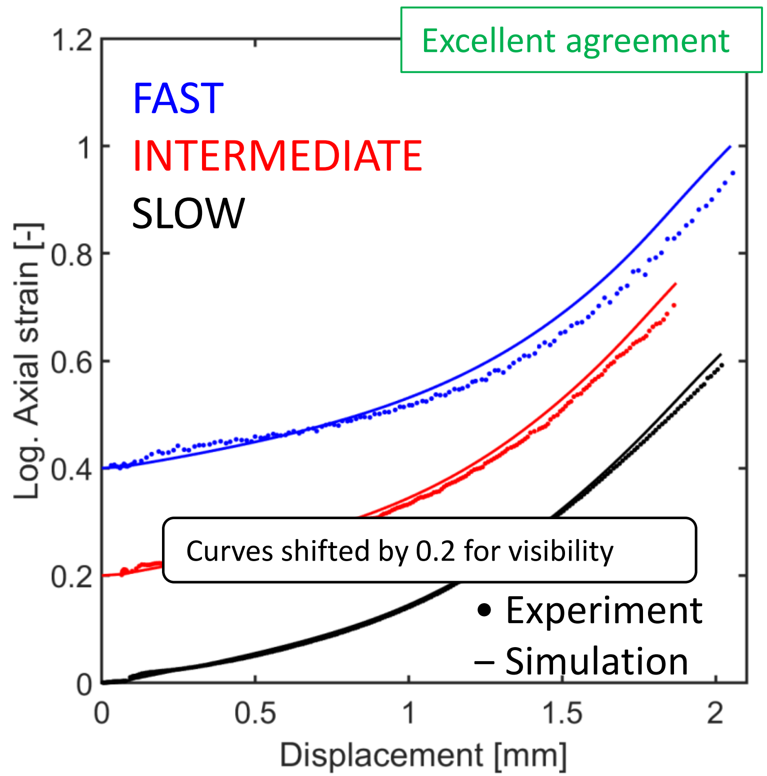

Performance of Trained Model

Li, Roth and Mohr (2019)

- Training data for quasi-static loading @ ~10^{-3}/s (six experiments)

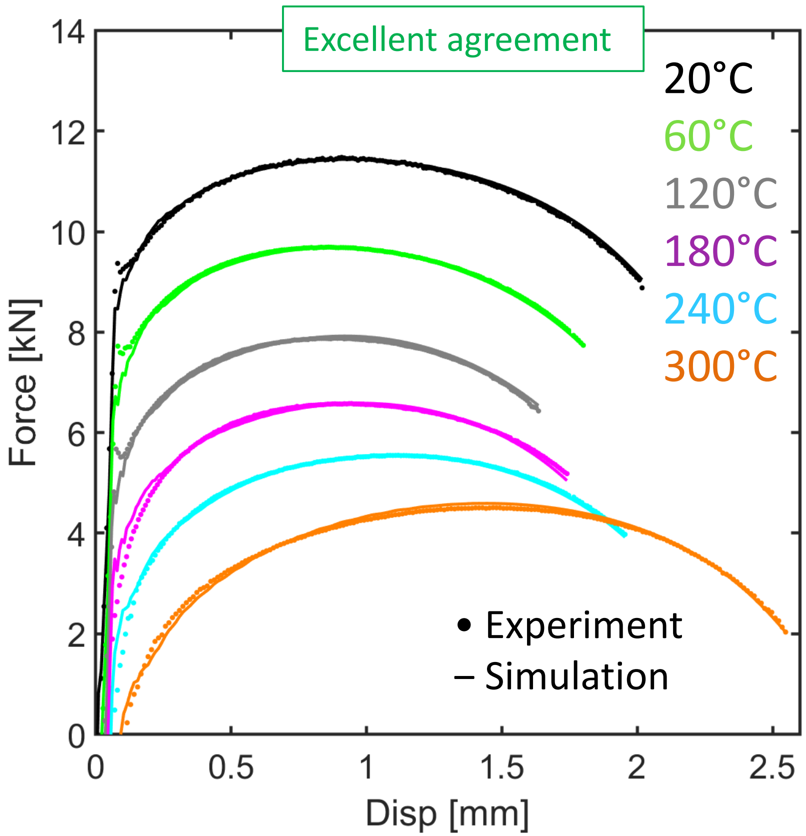

Curves shifted by -1.5kN for visibility

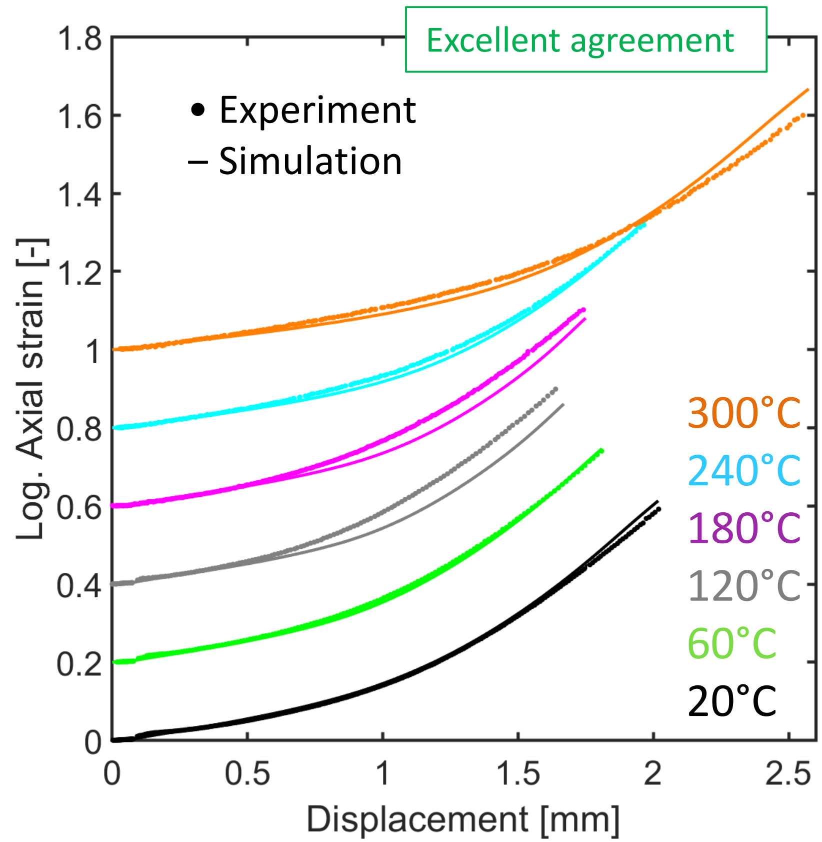

Curves shifted by 0.2 for visibility

Validation of Trained Model

Li, Roth and Mohr (2019)

- Training data for loading @ room temperature (three NT6 experiments)

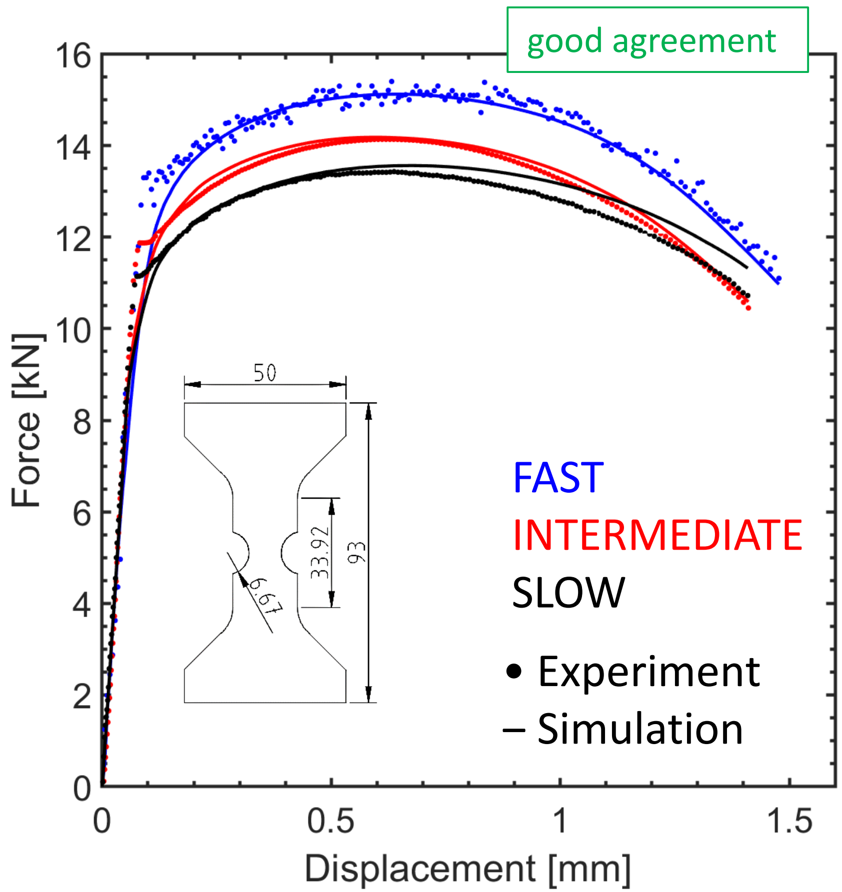

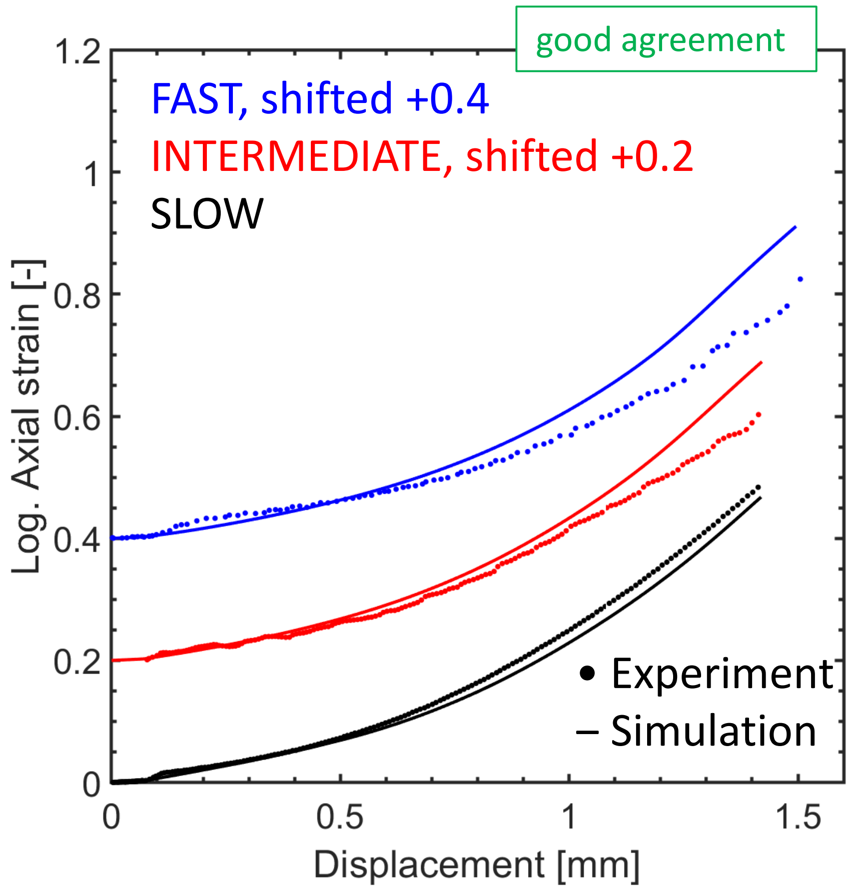

Hardening model identified through Machine Learning

Li, Roth and Mohr (2019)

Quasi-Static (10^{-3}/s)

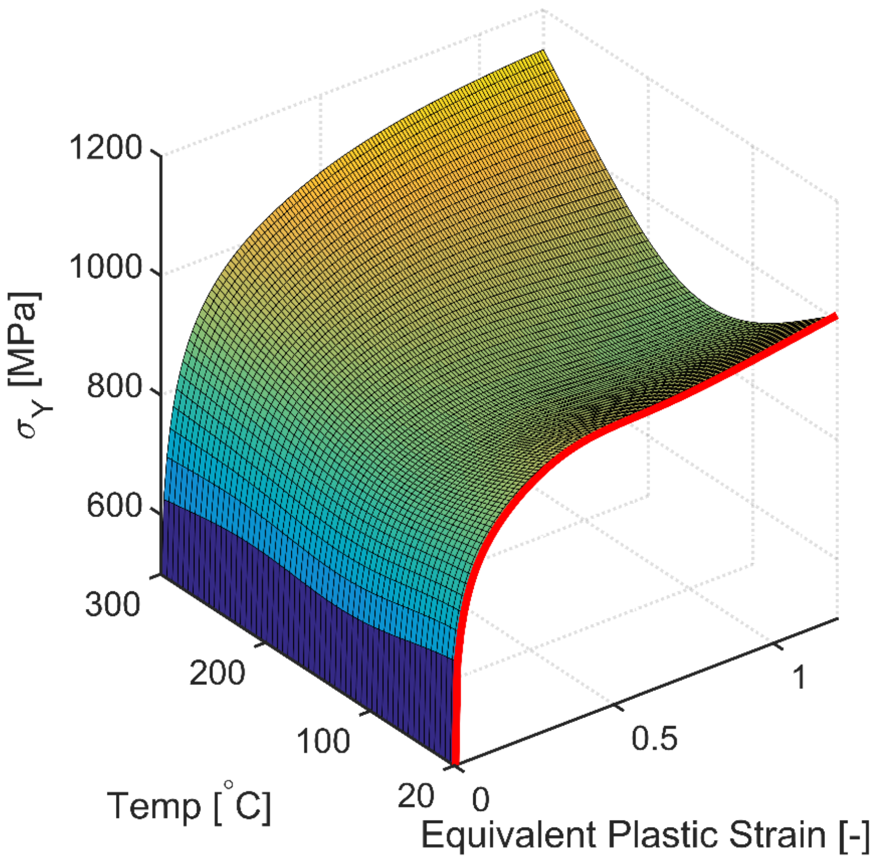

T=20°C

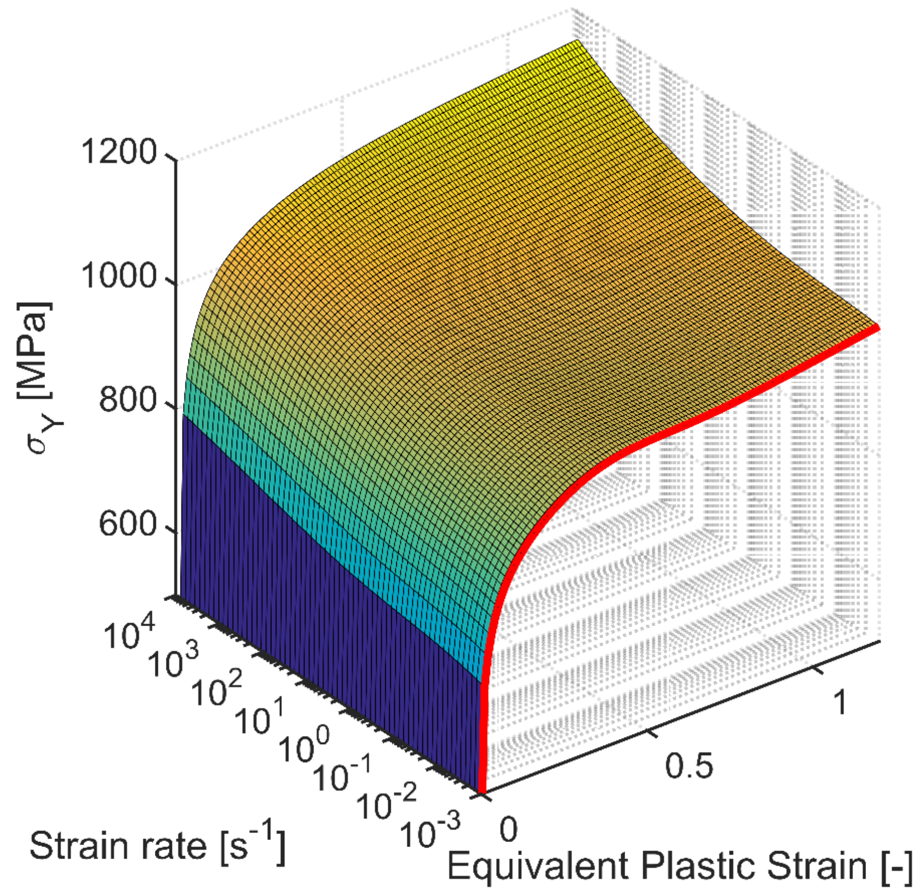

Loading Paths to Fracture

for quasi-static experiments on DP780 steel

Li, Roth and Mohr (2019)

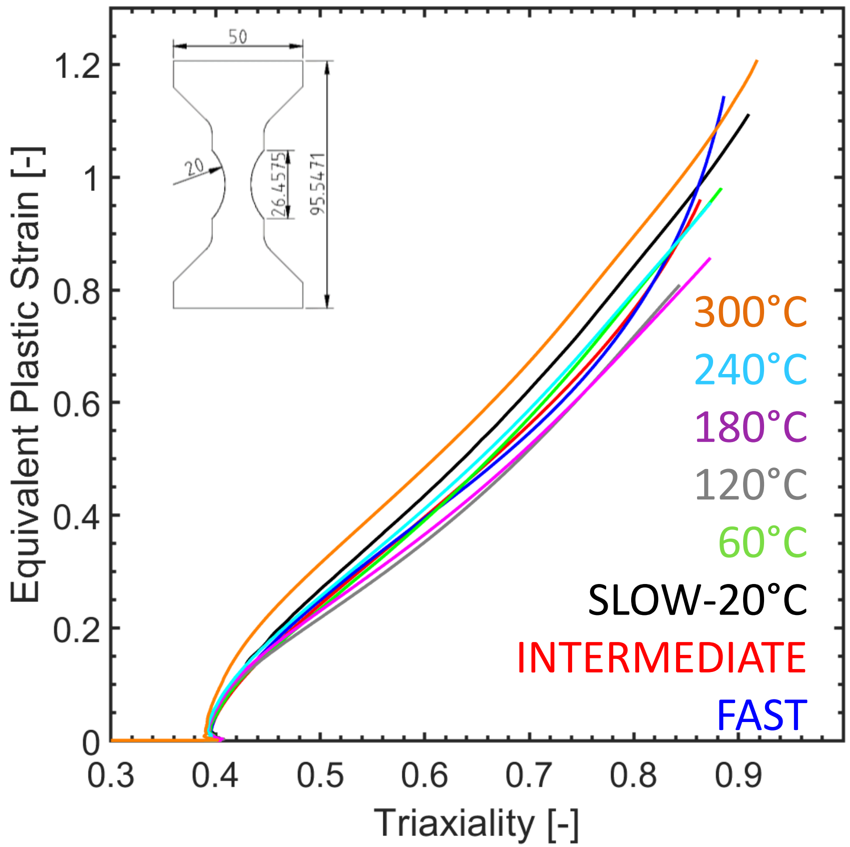

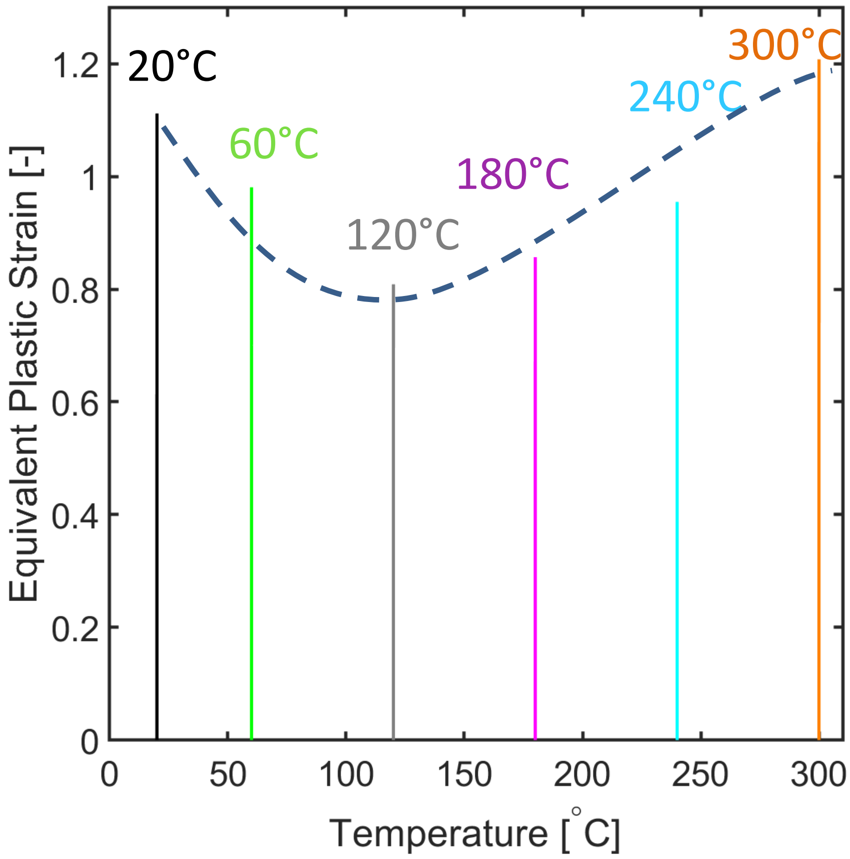

- **Non-monotonic effect of temperature on fracture strain!**

Outlook

Jordan, Gorji and Mohr (2019)

- Application to other materials (e.g. polypropylene)

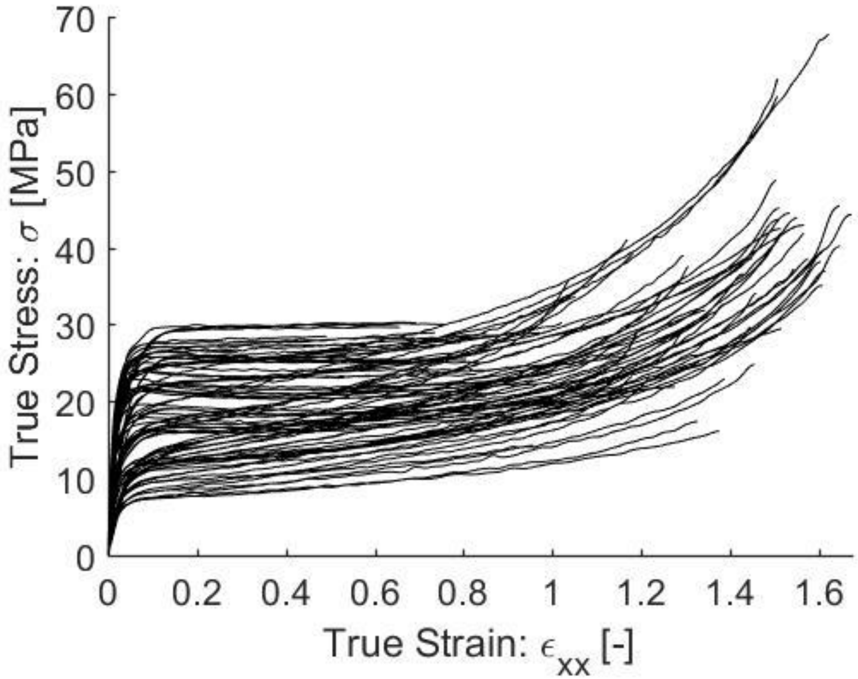

more than 100 experiments for different temperatures and strain rates

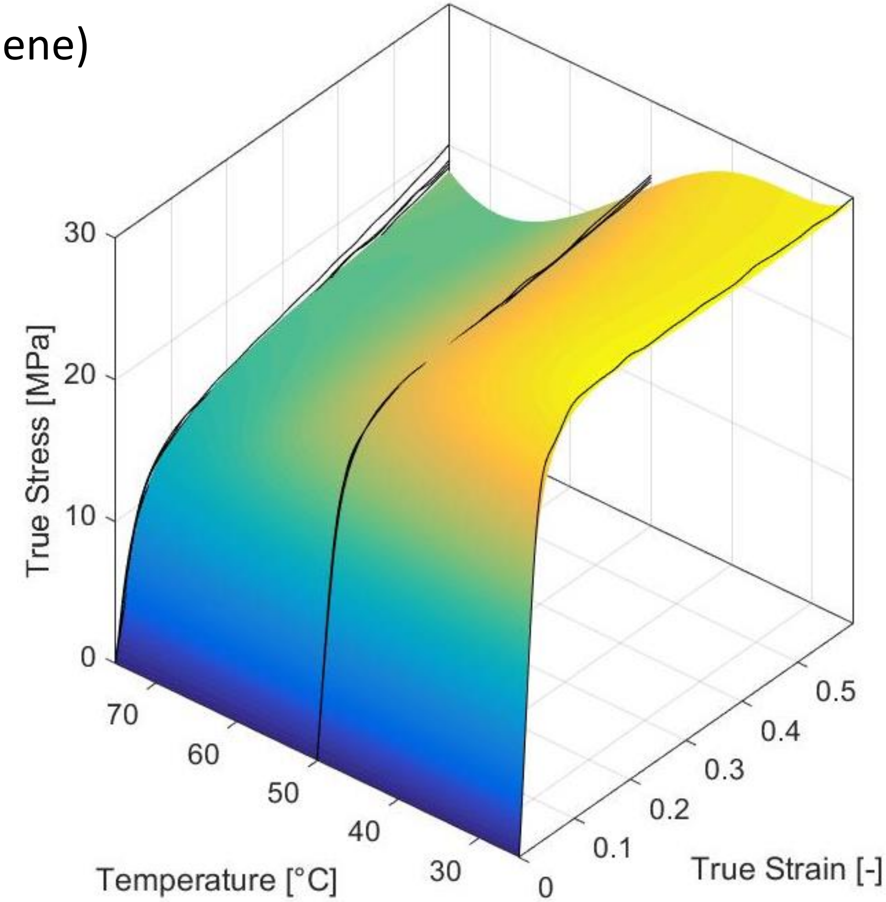

Machine-learning identified model

… but we need “big data”!

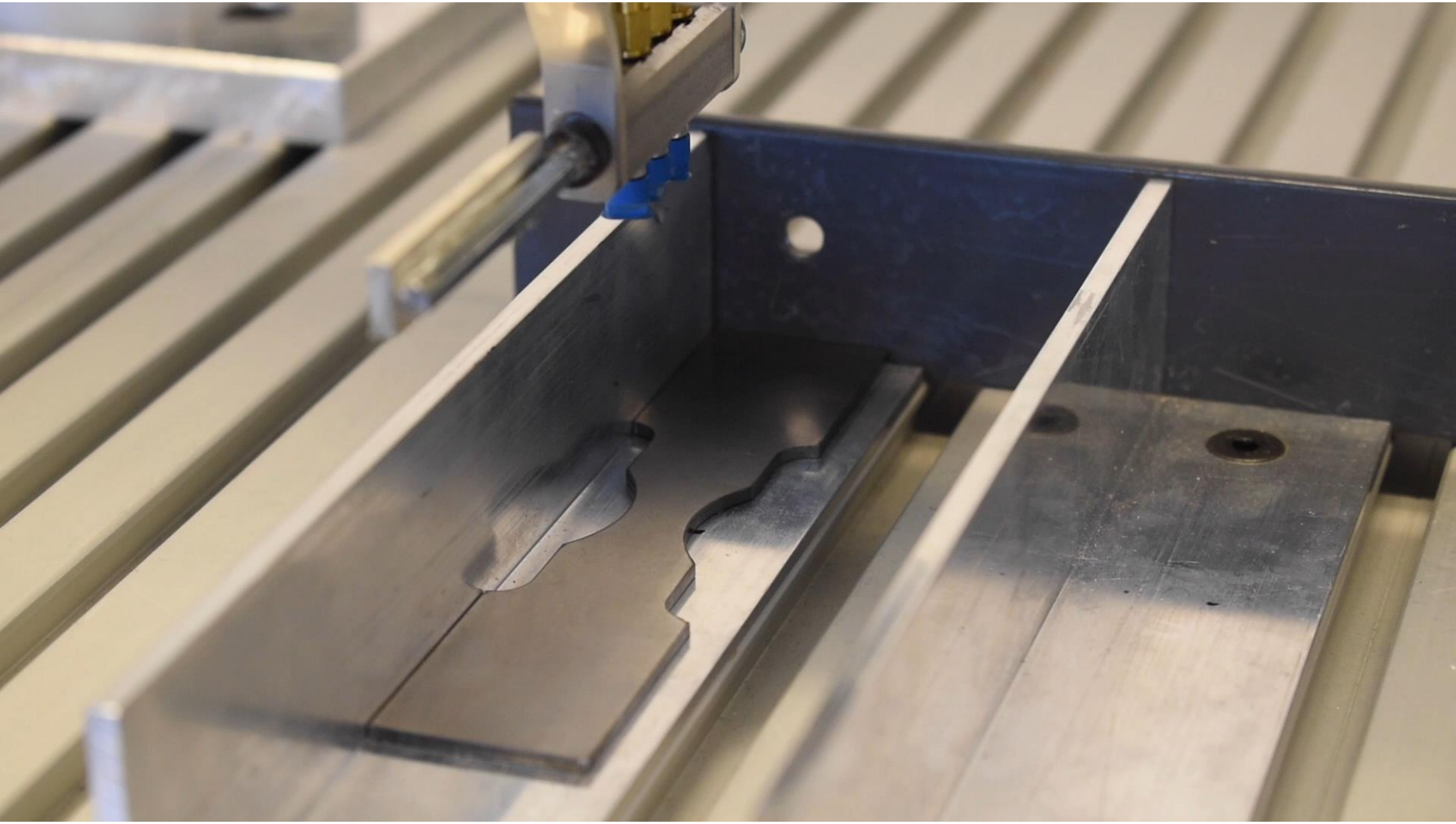

Summary

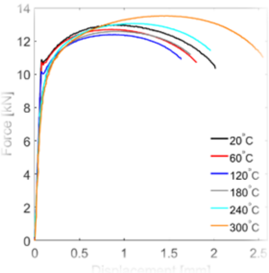

- Demonstrated non-monotonic effect of the temperature on the plasticity of dual phase steel

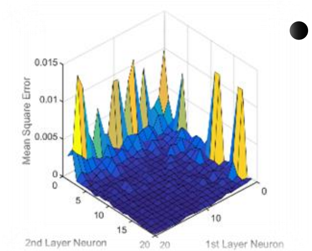

- Proposed a Neural-Network based temperature/strain rate term as a substitute of the classical Johnson-Cook term

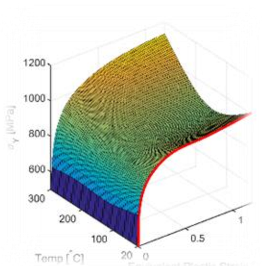

- Implemented the model into material user subroutine of Abaqus/explicit, trained & validated the model

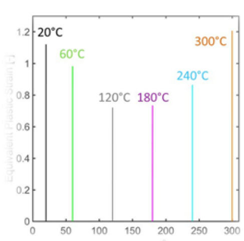

- Observed non-monotonic effect of the temperature on the fracture strain at RT

Acknowledgement

- **Important contributors**

V. Grolleau
• Visiting Prof.

C. Roth
• Scientist

M. Gorji
• Scientist

E. de Best
• Engineer

G. Gary
• Collaborator

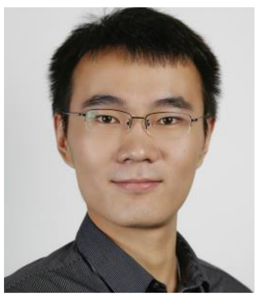

X. Li
• PhD Student
(2017-today)

B. Jordan
• PhD Student
(2018-today)

M. Dunand
• PhD Student
(2009-2013)

S. Marcadet
• PhD Student
(2011-2015)

B. Erice
• Postdoc
(2014-2016)

- **Funding: MIT/ETH Industrial Fracture Consortium (2007-today)**

Selected References

1. Dunand, M. & Mohr, D., 2014. Journal of the Mechanics and Physics of Solids Effect of Lode parameter on plastic flow localization after proportional loading at low stress triaxialities. *Journal of the Mechanics and Physics of Solids*, 66, pp.133–153. http://dx.doi.org/10.1016/j.jmps.2014.01.008
2. Erice, B., Roth, C.C. & Mohr, D., 2017. Stress-state and strain-rate dependent ductile fracture of dual and complex phase steel. *Mechanics of Materials*, pp.1–22. http://dx.doi.org/10.1016/j.mechmat.2017.07.020
3. Mohr, D. & Marcadet, S.J., 2015. Micromechanically-motivated phenomenological Hosford-Coulomb model for predicting ductile fracture initiation at low stress triaxialities. *International Journal of Solids and Structures*. https://doi.org/10.1016/j.ijsolstr.2015.02.024
4. Roth, C.C. & Mohr, D., 2015. Ductile fracture experiments with locally proportional loading histories. *International Journal of Plasticity*, 79, pp.328–354. http://dx.doi.org/10.1016/j.ijplas.2015.08.004
5. Roth, C.C., Gary, G. & Mohr, D., 2015. Compact SHPB System for Intermediate and High Strain Rate Plasticity and Fracture Testing of Sheet Metal. *Experimental Mechanics*, 55(9), pp.1803–1811. Roth,
6. Roth, C.C. & Mohr, D., 2014. Effect of strain rate on ductile fracture initiation in advanced high strength steel sheets: Experiments and modeling. *International Journal of Plasticity*, 56, pp.19–44. https://doi.org/10.1016/j.ijplas.2014.01.003
7. Fras, T., Roth, C.C. & Mohr, D., 2018. Fracture of high-strength armor steel under impact loading, International Journal of Impact Engineering, 111, pp. 147-164, https://doi.org/10.1016/j.ijimpeng.2017.09.009
8. Grolleau, V., Roth, C.C., Lafilé, V., Galpin, B. & Mohr, D., 2019. Loading of mini-Nakazima specimens with a dihedral punch: Determining the strain to fracture for plane strain tension through stretch-bending, International Journal of Mechanical Sciences, 152, 329-345, https://doi.org/10.1016/j.ijmecsci.2019.01.005
9. Roth, C.C. & Mohr, D., 2018. Determining the strain to fracture for simple shear for a wide range of sheet metals, International Journal of Mechanical Sciences, 149, 224-240, https://doi.org/10.1016/j.ijmecsci.2018.10.007